

DEVELOPMENT OF ELECTROMAGNETIC-BASED HAPTICS DISPLAY WITH HEIGHT VARIATION

by

Hilarius Prin Pujianto

A Thesis Submitted in Partial Fulfillment of the Requirements for the Degree of
Master of Engineering in Mechatronics

Examination Committee: Prof. Manukid Parnichkun (Chairperson)
Dr. Mongkol Ekpanyapong
Dr. Pisut Koomsap

Nationality: Indonesian
Previous Degree: Bachelor of Electrical Engineering
Satya Wacana Christian University
Indonesia
Scholarship Donor: AIT Fellowship

Asian Institute of Technology
School of Engineering and Technology
Thailand
May 2022

AUTHOR'S DECLARATION

I, Hilarius Prin Pujianto, declare that the research work carried out for this thesis was in accordance with the regulations of the Asian Institute of Technology. The works presented in it are my own and have been generated by me as the result of my own original research, and if external sources were used, such sources have been cited. It is original and has not been submitted to any other institution to obtain another degree or qualification. This is a true copy of the thesis, including final revisions.

Date: January 20, 2022

Name: Hilarius Prin Pujianto

Signature:



ACKNOWLEDGMENTS

In finishing this final report, I'd like to thank my advisor, Prof. Manukid Parnichkun, for his encouragement and support during the postulation process, as well as for allowing me to submit my master's thesis to the Asian Institute of Technology. I'd like to express my gratitude to Dr. Mongkol Ekpanyapong and Dr. Pisut Koomsap, members of my examination committee, for their valuable and crucial suggestions.

In addition, the I-S-E members for the documentation direction and all of the helps they provided. I'd also like to express my gratitude to my Advanced Robotics Laboratory colleagues and other ISE colleagues for their excellent advice. I would also like to express my gratitude to AIT and Thailand for allowing me to pursue my master's degree at AIT. Finally, express my gratitude to my family and community in Indonesia for their assistance in completing the assignment successfully.

ABSTRACT

This research enhances the haptics display that usually functioned as a dynamic Braille Letter, with an ability to vary the dynamic pins' height. These height variations can be utilized to deliver more kinds of information, for example the color, density, graphic trend, etc. There are nine cells of moving pins developed in this research. The movement range of the pins is between 0 to 10mm, with the distance among the pins is around 14mm.

There are ferromagnetic sheet walls outside each cell to redirect the magnetic field so that the interaction among permanent magnets is reduced since the distance among pins is very close. Every cell consists of a pair of coils and permanent magnets as the main components. The system's working principle is by flowing different amounts of an electric current inside the lower and upper coil in the cell. The permanent magnet moves up or down along with the pin according to the received magnetic force produced by the coils.

The electric current regulation process is done by utilizing a MOSFET for each coil driver. The electric current amount depends on the input that is converted to 8 bits digital value then to analog (voltage) and sent to the MOSFET. A braking mechanism driven by the servo motor stops the pin movement and makes the power for the coils can be turned off to avoid excessive heat of the coil and the pins can withstand 0,5N of load on it. The repeatability rate of the system is stated with Standard Deviation value 0.106 and Pooled Relative Standard Deviation 2%. The accuracy of the system is 76%. The performance is affected by the coil winding and friction among the parts.

CONTENTS

	Page
ABSTRACT	iv
LIST OF TABLES	vii
LIST OF FIGURES	viii
LIST OF ABBREVIATIONS	x
CHAPTER 1 INTRODUCTION	1
1.1 Background	1
1.2 Rationale	2
1.3 Problem Statement	2
1.4 Objective	2
1.5 Scope and Limitation	3
1.5.1 Scope	3
1.5.2 Limitation	3
CHAPTER 2 LITERATURE REVIEW	4
2.1 Definition and Concept of Haptic	4
2.2 BlindPad	5
2.3 Braille Letters	6
2.4 TanvasTouch Surface Haptics	7
2.5 Mid-air Haptic for Rendering 3D Shapes	9
2.6 Colour Image to Grayscale Image Conversion	12
2.7 Lorentz Force Application (Railgun)	13
2.8 Solenoid as Electromagnetic Actuator	16
2.9 Electric Current Regulator	17
2.10Chapter Summary	19
CHAPTER 3 METHODOLOGY	20
3.1 Working Step	20
3.2 Hardware Design	21
3.2.1 Working Process of Haptics Display	21
3.2.2 Block Diagram of The System	22
3.2.3 Actuator Board Design	23
3.2.4 Bridge Board	27

	Page
3.2.5 Digital to Analog Converter	29
3.2.6 Voltage Controlled Current Regulator	31
3.3 Controller Design	34
3.3.1 General Purpose Input/Output (GPIO)	34
3.3.2 Graphical User Interface (GUI)	37
3.4 System Integration	39
3.5 Chapter Summary	41
CHAPTER 4 RESULTS AND DISCUSSION	42
4.1 Repeatability	42
4.2 Accuracy	47
4.2.1 Accuracy of Reference Value	48
4.2.2 Accuracy of Estimated Value	48
4.2.3 Accuracy of Combined Reference Value	49
4.2.4 Accuracy of Combine Estimated Value	50
4.3 Chapter Summary	50
CHAPTER 5 FUTURE WORK AND RECOMMENDATION	52
REFERENCES	54

LIST OF TABLES

Tables	Page
Table 3.1 Bridge Board Input List	28
Table 3.2 Bridge Board Output List	29
Table 3.3 Raspberry Pi GPIO List	36
Table 4.1 First Repeatability Test Result	43
Table 4.2 Standard Deviation of First Test	44
Table 4.3 Second Repeatability Test Result	44
Table 4.4 Standard Deviation of Second Test	45
Table 4.5 Repeatability Third Test Result	45
Table 4.6 Standard Deviation of Third Test	46
Table 4.7 Repeatability Fourth Test Result	46
Table 4.8 Standard Deviation of Fourth Test	47
Table 4.9 Accuracy of Reference Value Test Result	48
Table 4.10 Accuracy of Estimated Value Test Result	49
Table 4.11 Accuracy of Combined Reference Value	49
Table 4.12 Accuracy of Combined Estimated Value	50

LIST OF FIGURES

Figures	Page
Figure 2.1 Joystick for Game Console	4
Figure 2.2 BlindPad	5
Figure 2.3 Configuration of Membrane Pulling and Pushing	6
Figure 2.4 Braille Alphabets	6
Figure 2.5 TanvasTouch Hardware	7
Figure 2.6 Implementation of Electro-adhesion-based Surface Haptics	8
Figure 2.7 TanvasTouch Software Interface	9
Figure 2.8 Stratos Explore by Ultrahaptics Ltd.	10
Figure 2.9 Focal Point from Ultrasound Wave	10
Figure 2.10 Visual Representation of The Haptic Tactile Patterns	11
Figure 2.11 Particle-based Visualization of 3D Objects	12
Figure 2.12 Visual Performance Using Proposed Algorithm	13
Figure 2.13 Lorentz's Electromagnetic Force and Railgun Accelerator	14
Figure 2.14 Coil Induced Magnetic Field	15
Figure 2.15 Direct Acting Solenoid Valve	16
Figure 2.16 Actuation System Using Solenoid	17
Figure 2.17 Voltage Regulator Based Fixed Current Regulator	18
Figure 2.18 Voltage Regulator Based Variable Current Regulator	18
Figure 2.19 Transistors Based Current Regulator	18
Figure 3.1 Working Step	21
Figure 3.2 Working Process of The System	22
Figure 3.3 Block Diagram of The System	22
Figure 3.4 Single Unit of Pin Movement Mechanism	23
Figure 3.5 Coil Winding	24
Figure 3.6 Single Cell with Ferromagnetic Sheet Outside	24
Figure 3.7 3D Printed Single Cell Parts	25
Figure 3.8 Three and Nine Cells Actuating Board	26
Figure 3.9 Brake Mechanism	27
Figure 3.10 Bridge Board	27

Figures	Page
Figure 3.11 Digital to Analog Converter Circuit	30
Figure 3.12 Driver Board	31
Figure 3.13 Current Regulator Circuit	32
Figure 3.14 Pins at Maximum Height	34
Figure 3.15 Raspberry Pi GPIO	35
Figure 3.16 Graphical User Interface	38
Figure 3.17 Last Recent Values File	38
Figure 3.18 Measurement Process	40
Figure 3.19 Text File of Reference Values	41

LIST OF ABBREVIATIONS

ASCII	= American Standard Code for Information Interchange
AWG	= American Wire Gauge
CCW	= Counter Clockwise
CW	= Clockwise
DAC	= Digital to Analog Converter
DC	= Direct Current
GPIO	= General Purpose Input/Output
GUI	= Graphical User Interface
IC	= Integrated Circuit
I/O	= Input Output
MOSFET	= Metal Oxide Semiconductor Field Effect Transistor
OPAMP	= Operational Amplifier
PLA	= Polylactic Acid
PRSD	= Pooled Relative Standard Deviation
PSD	= Pooled Standard Deviation
PWM	= Pulse Width Modulation
RSD	= Relative Standard Deviation
SD	= Standard Deviation
USB	= Universal Serial Bus

CHAPTER 1

INTRODUCTION

1.1 Background

The sense of touch is one of the senses possessed by humans to recognize the surrounding environment. Haptic technology allows the sense of touch to interact with computerized devices. This also can help those with special needs, for example the blind. By groping, someone can get information which are various textures, letters, and even a shape. One of the tools that can be used to enrich the interaction experience with a computer system or to help blind people receive information is an electromagnetic-based haptic display.

The electromagnetic-based haptic display is a board on which there are many pins that can go up and down. This set of pins can form a specific pattern so that it is understood by the user as different information, such as braille letters. In principle, one layer of the board has many slots in the form of a coil for magnetic pins, where when the coil is energized, the magnetic pin will move up or down to the maximum. The movement of this group of magnetic pins makes a difference in height with other groups of magnetic pins whose coils are activated in different ways so that when they are touched, they will be understood as a certain pattern that can be interpreted as information.

Information delivery enhancement can be achieved by enriching the ability of a haptics display to vary the height of the pin on it. The height variation is a representation of an image to be understood by the user, especially for those who have a visual impairment. This enhanced haptics display hopefully can enlarge information delivery from any information broadcaster, for example the government and television station, to people who have a disability in enjoying video and audio data at the same time. In combination with an image conversion system, electromagnetic-based with height variation haptics display will be able to display dynamic information according to the converted image.

In this research, an electromagnetic-based haptic display will be made with two layers of coil boards. This allows each magnetic pin to move up and stop at a certain height, not always at its maximum height. The value of the electric current that is applied to each coil both at the bottom and top layers will cause the magnetic pin to stop at a

certain height. With this capability, a more diverse range of information can be presented, such as graph trends, regional topographic images, etc.

1.2 Rationale

Advances in technology allow information to be sent quickly. Speed of delivery is not a guarantee that information will be well received. Appropriate presentation of information also plays an important role so that the meaning of information can be understood properly. Presentation of information with multiple heights of electromagnetic-based haptics display can be done with more variations and allows the meaning of the information to be presented accurately, especially for those with special needs, such as blind people.

1.3 Problem Statement

Varying pin height is the main ability of the enhanced electromagnetic-based haptics display. The attractive and repulsive force between a permanent magnet and an electromagnet must be driven to get the desired height and force. The making of induction coils as electromagnetic force producers needs to pay attention to the dimension, for example the diameter, number of turns, and the length of the coil.

It takes digital data processing in the controller to be sent to the analog driver. The analog driver will regulate the flow of electric current in the coil, which causes the magnetic pin to move up to a certain point as the system output. In other word, the pair of coils must be energized with an appropriate proportion of voltage and electric current. This mechanism must also be constructed so that as few cables as possible are used to connect between the controller and analog driver, as well as between the analog driver and actuator.

Electromagnetic-based haptics display must have a compact design to be comfortable to use in fulfilling its function. Modelling using software and the realization of this modelling is possible using a 3D printer.

1.4 Objective

The purpose of this research is to create an electromagnetic-based haptic display that has the ability to adjust the height of each magnetic pin to stop at a certain point according to the data sent. Current flow regulation in a pair of coils on each pin is implemented to achieve this goal.

In order to control the current flow in the coil, digital data processing is carried out to provide input to the analog driver. The combination of the current values in the coil will affect the height of the magnetic pin as the output.

1.5 Scope and Limitation

1.5.1 Scope

- Controller programming to process the input as digital data and output it as an analog value as the analog driver input
- Analog driver design to regulate current flow in the coil that controls the movement of the magnetic pins.
- The design of the magnetic pinboard with the target distance between pins is 1,5 cm.
- Adjustment of current flow in the coil and hardware mechanism so that the magnetic pin can withstand a load of 0,5N.
- Adjustment of the system to maintain the accuracy of the pin's position at the 4 points of the height of the pin.
- Adjustment of the system to achieve repeatability of the pin's position at the 4 points of the height of the pin.

1.5.2 Limitation

- The size of the magnetic pin array created is 3 x 3 pins, of which the total number of magnetic pins is nine due to the limited budget.
- Variation of the magnetic pin height using digital to analog conversion from 0 – 1cm.

CHAPTER 2

LITERATURE REVIEW

The designed system consists of an input device, controller, and output device. The basic knowledge and reference are mentioned and explained in this chapter. The whole idea is related to the haptics display and the using of the electromagnetic as an actuator. The flowing electric current control inside certain coil is the main topic to build the haptics display in this research.

2.1 Definition and Concept of Haptic

Haptic technology (Haptics) is a specific technology that simulates tactile sensations. Felix G. Hamza-Lup and his friends, on their paper, explained some words related to haptics. A professor from the University of Leipzig named Ernst Heinrich was the person who initiated the research on Haptics. This research was then continued by Ivan Sutherland through his thesis. Ivan argued that human sensory movements make information assimilated under the human consciousness. Starting from the mid-1990s, the haptic became increasingly popular with the presence of joystick for games on certain game consoles, as shown in Figure 2.1.

Figure 2.1

Joystick for Game Console



Communication built through touch is an advantage of haptic technology. Haptics makes the digital world, which is currently known as virtual reality, can be treated as in the real world. Haptic allows simulations to be carried out as closely as possible to the original conditions, for example being used by technicians before designing components, doctors before operating on real patients, pilots before flying a real airplane, etc.

Haptics is applied in many fields, such as computers and video games, telecommunications, virtualization, remote control, simulators, etc. In principle, haptic technology can be used to interact between humans and computers. This means that through haptic technology, two-way communication is established between humans and computers. This kind of communication can be felt increasingly real day by day along with the development of haptics. However, not a few haptic technologies provide only a one-way response to users, for example, the haptics display.

2.2 BlindPad

BlindPad is an example of a haptic display developed from 2014 to 2017 (BlindPad: Project Final Report 2017). This tool was made for visually impaired persons who find a difficulty to obtain increasingly complex graphic content that normally can be easily enjoyed by people with normal vision.

BlindPad consists of 192 pins (12x16) with a distance of 8mm between pins (Figure 2.2). On the actuator, BlindPad uses the latch principle to attach certain pins in the lower or upper position. The attractive and repulsive properties of a magnet are used in this board to create a pin locking system to stay up or down. This is achieved by such a membrane that holds its position in a concave or convex position (Figure 2.3). This membrane acts as a memory to save the last trigger, whether it is up or down position. A trigger on the coil will make the pin position switch from bottom to top or vice versa. When the magnetic pin is conditioned to the bottom or top position, energy is no longer required to hold the magnetic pin in position. This system has a fast response but only limited to 2 maximum positions, bottom or top.

Figure 2.2

BlindPad

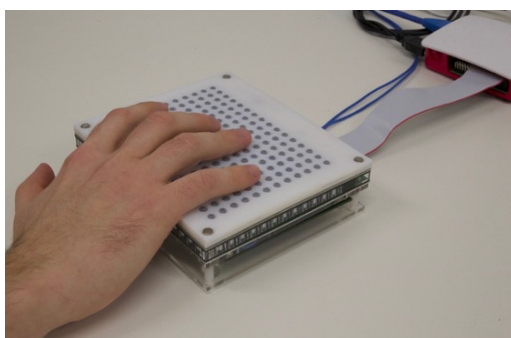
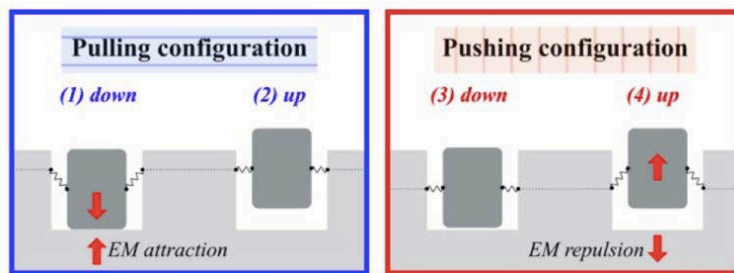


Figure 2.3

Configuration of Membrane Pulling and Pushing

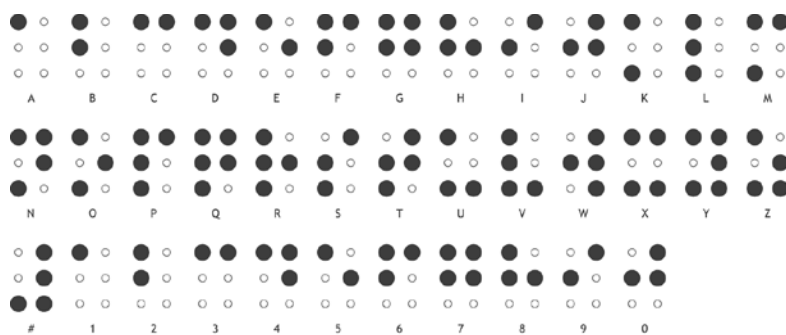


2.3 Braille Letters

Braille is a tactile writing system used by people who are visually impaired. This is according to the definition that is written on Wikipedia. Louis Braille invented this set of alphabets in the year 1824. Each alphabet consists of six dots arranged with three rows and two columns. The roughness of these six dots is conditioned to differ from one to another alphabet so that each alphabet has its own characteristic, as shown in Figure 2.4. People can grope the surface of the Braille Board to feel and understand what characters are on the board.

Figure 2.4

Braille Alphabets



The basic unit of this writing system is called the Braille cell, in which each cell consists of six embossed dots; three lines with two dots on each line. The six points can be arranged in such a way as to create 64 kinds of combinations. Braille is read from left to right and can represent alphabets, punctuation marks, numbers, musical signs, math symbols and more. The commonly used Braille font size is 0.5mm in height and 2.5mm of horizontal and vertical spacing between points in the cell.

There are some standardizations of the set of Braille Letters, usually different from one and another, but still in the same six-dot format. Extended version of Braille Letter is achieved by adding one more row at the bottom, so that the number of dots become eight, in order to gain more variations as ASCII (American Standard Code for Information Interchange) code does. This becomes one of the functions of BlindPad, that can be utilized as dynamic Braille Letter board to show a lot of letters continuously. These letters will be understood by its reader as a word or even sentence. This helps people who are visually impaired to be able to read. The principle of Braille Letter is adopted to this research not only for reading but also to inform another form of information such as particular contour or graphics trend.

2.4 TanvasTouch Surface Haptics

There are several types of surfaces that can be felt by groping it. Craig Shultz (2020), member of Haptic Experience Team in Tanvas Company, explained about TanvasTouch as a haptic device in delivering texture and roughness information. Tanvas is a company in Chicago USA that developed a development kit in multitouch screen display which has an ability in changing the friction on the screen while it is interacting with the movement of the finger when it is touched. This ability can be utilized to deliver information in the form of roughness or texture of any surface. This can be achieved by using synergy between developed software and hardware by Tanvas company. The development kit was already marketed and available for commercial use. The multitouch screen hardware developed by Tanvas is shown in Figure 2.5.

Figure 2.5

TanvasTouch Hardware



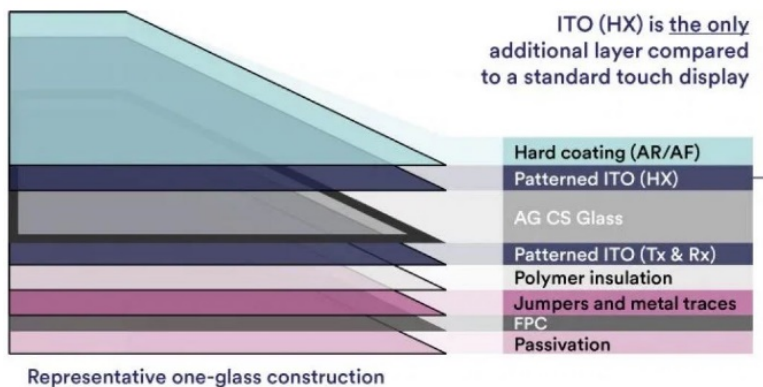
TanvasTouch uses the principle of electro-adhesion. Before, to develop any tactile engagement on a screen, a vibration named vibrotactile haptics was used. This was

difficult to localize to only give an effect of tactile sensations on particular area of the screen. Furthermore, the use of vibrotactile haptics became less efficient when it is applied onto larger screen size since it is mechanical based working principle. Instead of using vibrotactile haptics, a solid-state technology became the solution to address the problem of using mechanical way. Since it is a solid-state technology, it can be implemented in a display screen of any size and shape, as well as on other surfaces such as a glass or plastic enclosure.

The electro-adhesion principle uses force, not vibration, to produce tactile sensation, therefore there is no mechanical problem as in mechanical vibrotactile haptics use. In order to create tactile sensation on the screen, controlled voltage is applied to a transparent indium tin oxide (ITO) matrix. The layer of ITO is the only additional layer compared to a standard touch display. The implementation can be seen in Figure 2.6. By controlling the voltage applied to the ITO layer, the adhesion of the finger to the surface can be increased. This amplifies and modulates the naturally occurring friction force between the finger and smooth glass, leading to the feel of a range of textures.

Figure 2.6

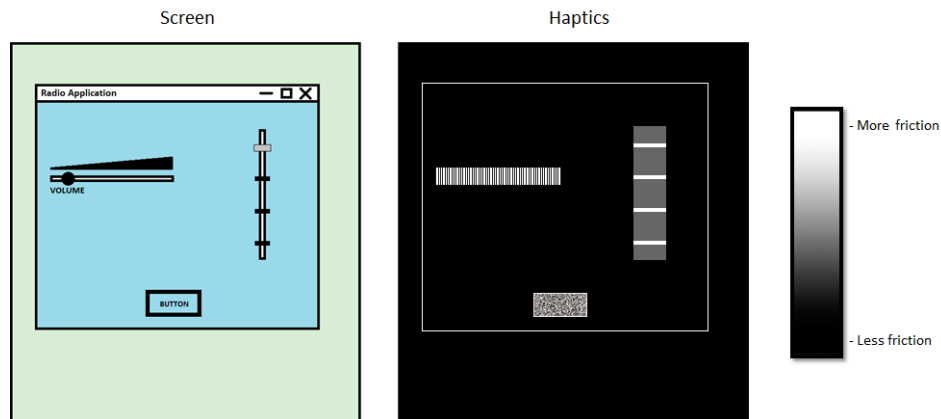
Implementation of Electro-adhesion-based Surface Haptics



This technology enables product designers or programmers to create unique, custom texture effects in an intuitive software development environment. As shown in Figure 2.7. that is the example of the software interface developed by Tanvas. This software can be used like drawing on a virtual canvas. The programmer is able to set specific friction force on a certain area. This area usually represented by some picture of components, for example picture of slide volume control, rotary knob for tuning any radio frequency, etc.

Figure 2.7

TanvasTouch Software Interface



Localizing tactile sensation makes the programmer can deliver texture and roughness of any surface, for example the texture and roughness of clothes. User can compare many textures and roughness from some clothes on the same screen display. ITO matrix here acts as actuator in combining electro-adhesion. Different adhesion between the surface of the screen and the finger produces different friction force. This localized force is received by the end users as information.

This surface haptics enriches a screen to be a multi-sensory device. By implementing the electro-adhesion, the user can experience the senses of sight, hearing, and touch simultaneously. Sense of sight when the user is seeing the displayed picture on the screen. Sense of hearing when the friction force between the finger and the equipped electro-adhesion screen produces such sound. Sense of touch by groping the screen to feel any kind of texture and roughness.

2.5 Mid-air Haptic for Rendering 3D Shapes

Vibrotactile sensation is able to be produced in the mid-air. Jonatan Martinez and his team (2019) from Ultrahaptics Ltd, United Kingdom, proposed an algorithm by using ultrasonic sound to produce vibrotactile effect in the mid-air. This algorithm turns ultrasound into virtual touch. Stratos Explore is one of the examples of the commercial product using this proposed algorithm. The picture of the Stratos Explore can be seen in Figure 2.8.

Figure 2.8

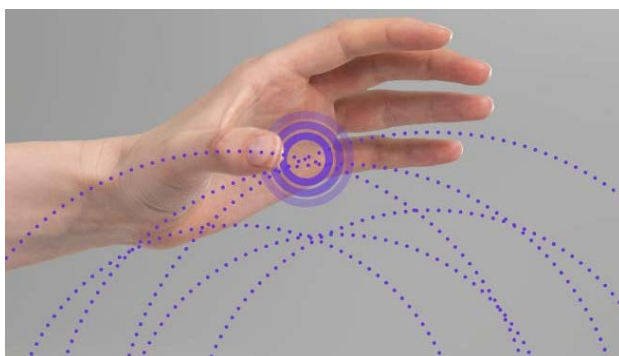
Stratos Explore by Ultrahaptics Ltd.



This device consists of many ultrasound speakers that emit high frequency sound. This frequency is too high to hear for the human. These speakers are put together to create an array on the surface of the device. Every ultrasound speaker can be controlled individually by the driver. Each individual speaker is triggered to emit an ultrasound at a very specific different time. The timing to trigger each speaker is defined by using patented proposed algorithms. These time differences mean the ultrasound waves arrive at the same point in space (in the mid-air), at the same time. The place where all the ultrasound waves coincide at one point is called the focal point. This focal point produces tactile effect on the hand. The illustration for focal point can be seen in Figure 2.9.

Figure 2.9

Focal Point from Ultrasound Wave

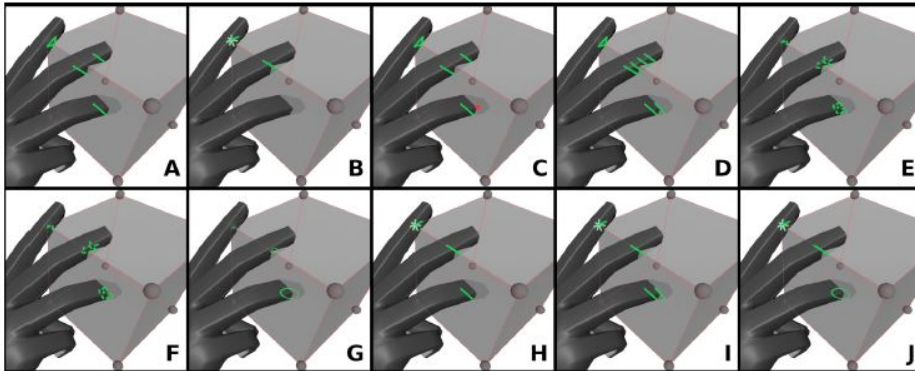


The focal points can be positioned in three-dimensional (3D) space programmatically in real time. The position can be changed from instant to instant. The combined ultrasound waves at focal point have enough force to create a tiny dent in human's skin.

This force creates a pressure point. This pressure point is used to create a vibration that touch sensors in human's hands can detect. Hand tracking device is used in order to detect the hand's position above the surface of the device. After being tracked at the exact position, then the system will place the focal point at a spot on the hand.

Figure 2.10

Visual Representation of The Haptic Tactile Patterns

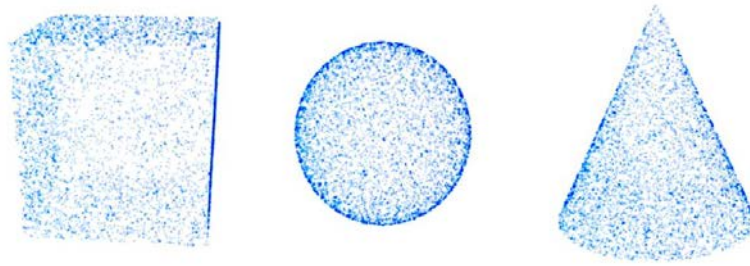


Tactile effects in the mid-air are created by moving the pressure points around the hand. The pressure points can be used to create wide range of tactile effects, from sculpting virtual lines and shapes to forming 3D controls in the mid-air. Haptic rendering methods by its visual representation can be seen in Figure 2.10. The rendering methods tried to create sensation felt by the hand by touch virtual 3D object start from only its intersection, features, until its solid form. This experiment did not consider the texture and weight of the rendered object.

Different objects were used in this experiment. They are cube, sphere, and cone. These objects were built by using group of pressure points that can be represented as particle-based object as shown in Figure 2.11. The objects have difference features which are felt by the hands when they are virtually touched. The experiment tried to utilize ultrasound wave to render 3D object in the mid-air that can be felt by touching the virtual object.

Figure 2.11

Particle-based Visualization of 3D Objects



This technology can be combined with virtual reality technology. A complete set of experience can be provided when people can see and touch the object virtually. This combination will make many simulations can be done without presenting the real thing to be practiced. The information that received by the users is in the form of such object which can be felt by groping it with their hands. Conditioned ultrasound waves are produced by the actuating unit of this device.

2.6 Colour Image to Grayscale Image Conversion

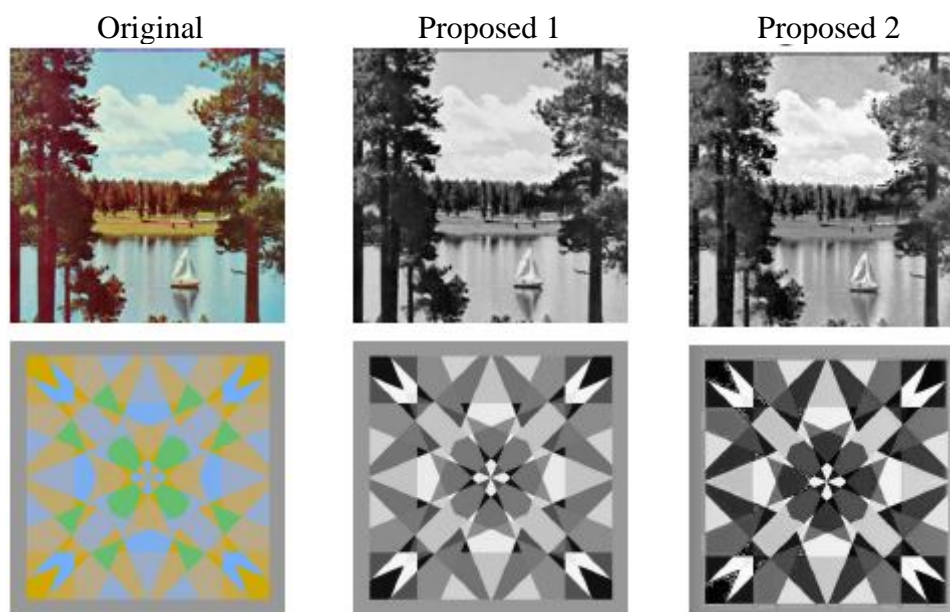
An image can be an input for the haptics display system. In order to give digital value in range, a colour image must be converted to grayscale image. Yi Wan and Qisong Xie (2016) from Lanzhou University, China, on their paper, explained a framework to convert RGB (Red Green Blue) colour image to grayscale image. In this research, two methods were proposed to achieve the goal of a colour to grayscale image conversion which is as much contrast information as possible. Fewer luminance representation bits cause poorer contrast in grayscale image than the original colour one.

The original image in Red Green Blue (RGB) colour format usually converted by using an approach described as $I = \alpha_r R + \alpha_g G + \alpha_b B$ where the non-negative summation of the coefficients α_r , α_g , and α_b results in 1. There are many methods proposed before Yi Wan's and Qisong Xie's research to determine the value of those coefficients. Nevertheless, in their research they presented a framework that tries to find the optimal line direction so that the projections from all colour pixel vectors are the most widely spread-out. This new framework will adaptively choose the vector α so as to make full use of all the grayscale levels. Toward this goal, the entropy of the histogram of all the projected I values are used.

In principle, the conversion of colour image to grayscale image in this research uses two-stage framework. In the first stage, a direction vector is chosen adaptively and projection of all colour pixel vectors onto this direction is done. The direction is chosen by maximizing the entropy of the histogram of all the projected points. This allows for better utilization of the full grayscale levels and performs better than the non-adaptive methods. Furthermore, in the second stage, to make full use of the grayscale levels, a simple histogram specification method is presented so that all the grayscale level are evenly used by all the pixels. The results of the methods are shown in Figure 2.12.

Figure 2.12

Visual Performance Using Proposed Algorithm



Better grayscale representation can be seen obviously because of high contrast as a result of good grayscale conversion. The value of each pixel or group of pixels from the conversion of a color photo to grayscale can provide input that is more suitable for haptics display as a representation of the desired color. This makes thing possible to utilize developed haptics display directly connected to image converter system.

2.7 Lorentz Force Application (Railgun)

Railgun is a kind of weapon that utilizes the principle of electromagnetic force to launch a projectile in high velocity. Ching-Chuan Su (2006), from National Tsinghua University, Hsinchu, Taiwan, presented mechanisms for the longitudinal recoil force in

railguns based on the Lorentz Force Law. When a current carrying conductor is placed in a magnetic field, it will be subjected to an induced force given by

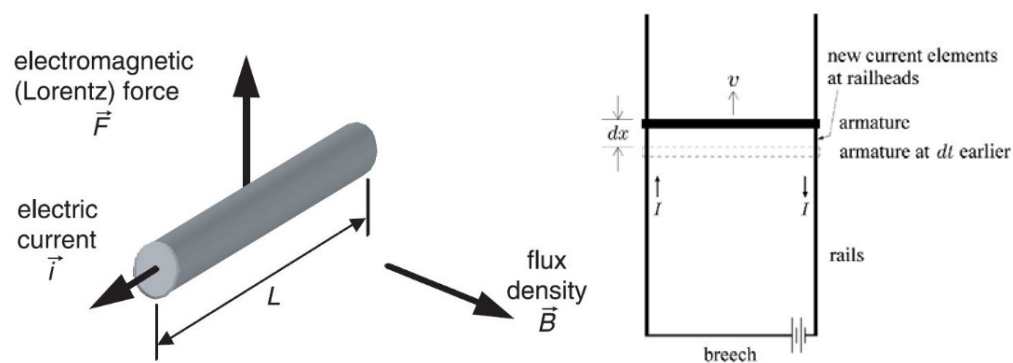
$$\vec{F} = \vec{i} \times \vec{B}$$

where \vec{F} is the force vector, \vec{i} is the current vector, and \vec{B} is the magnetic flux density. The force is called the electromagnetic force or the Lorentz force. If a conductor of length L carrying constant current i is placed in a constant field B , as shown in Figure 2.13, the magnitude of the resultant Lorentz force \vec{F} exerted by the field B on the conductor is

$$F = |\vec{F}| = BLi$$

Figure 2.13

Lorentz's Electromagnetic Force and Railgun Accelerator



Railgun utilizes magnetic force to accelerate an armature to move along two parallel rails on which it is placed, as shown in Figure 2.6. The current I flowing on the loop formed by the rails, the armature, and the breech generates a magnetic vector potential and a magnetic field. The current-carrying armature experiences a magnetic force, which tends to accelerate the armature to move along the rails. The effect of the motion of the armature is the new current elements located on the rails behind the armature. Ching-Cuan Su in this paper proposed a mechanism to account the longitudinal recoil force exerted on the rails of railgun accelerators.

In order to generate a desired magnetic field, or equivalently, a desired magnetic flux density, there are two methods that can be used. One is to use a permanent magnet and the other is to utilize the Biot–Savart law. A long (infinite), straight, current carrying

conductor induces a magnetic field around the conductor. The flux density at a perpendicular distance from the conductor is

$$B = \frac{\mu_r \mu_0}{2\pi r} \cdot i$$

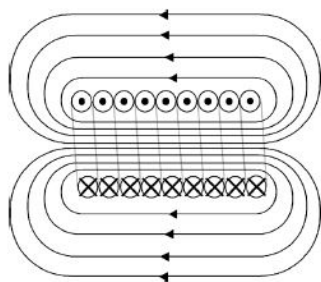
where i is the electric current. If we bend the straight current carrying conductor into a helical coil (solenoid) with N turns, it will induce a corresponding magnetic field as shown in Figure 2.14. If the length of the coil L is much greater than its diameter, the flux density follows the right-hand rule and the magnitude inside the coil is approximately

$$B = \mu \frac{N}{L} \cdot i$$

where $\mu = \mu_r \cdot \mu_0$ is the permeability of the material inside the coil and i is the current through the winding. This field can be intensified by inserting a ferromagnetic core into the solenoid by increasing the permeability. Coil induced magnetic fields is widely utilized in electromagnetic devices for generating controlled magnetic fields and are often referred to as electromagnets.

Figure 2.14

Coil Induced Magnetic Field



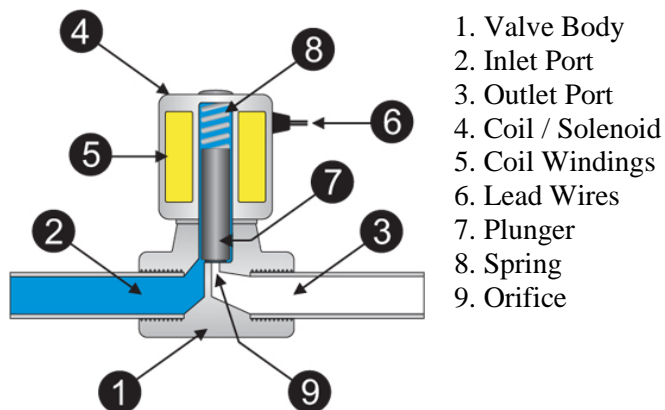
In this haptics display development, coil induced magnetic field result of a pair of coils is used to affect permanent magnet (pin) movement so that the permanent magnet can move and stop at certain height by adjusting the electric current flowing in the coils. The electricity will be regulated using voltage and current regulator controlled by analog value obtained from digital value conversion in the controller.

2.8 Solenoid as Electromagnetic Actuator

Solenoid is known as one of the electromagnetic applications. Solenoids are usually used in linear and rotary actuations for valves, relays, and switches due to the large force that the solenoids can produce at short stroke length whilst having a low reaction time. One of the common solenoids that often be used is direct acting solenoid valve as shown in Figure 2.15. Syed Zainal Abidin Syed Kamarul Bahrin and his team (2016), from Universiti Tenaga Nasional in Malaysia, used solenoids to build robotic hand. Solenoid characteristic is very ideal to provide strong grasping strength and fast speed motions.

Figure 2.15

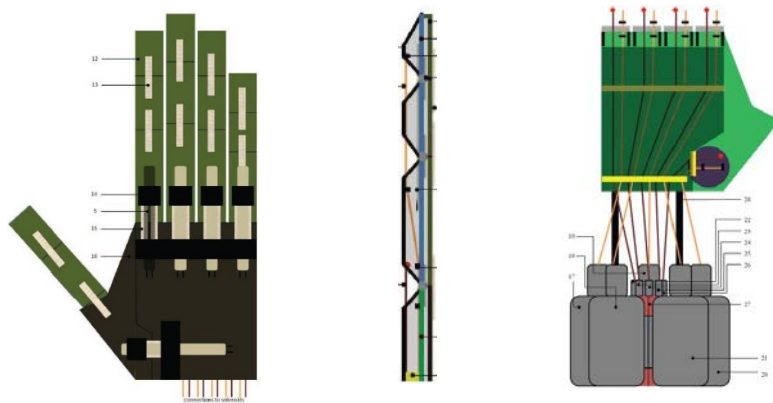
Direct Acting Solenoid Valve



The principle of the robotic hand built by using a group of solenoids is to connect high tension string in certain points of each finger to be able to imitate the palm of the human. The detail of the hardware is shown in Figure 2.16. The solenoid actuators can generate the fingers' motions through a combination of string-hinge mechanism. Each finger needs two solenoids to create a full hooking or grasping action. In conclusion from the paper, the solenoid actuators have the ability to create decent fingers' motions that are fast, responsive, and have strong grasping strength.

Figure 2.16

Actuation System Using Solenoid



The developments of solenoid designs have improved over the past few years with multistage coils and new plunger designs. These improvements allow the solenoid to have a longer displacement while maintaining a decent, same or higher amount of force. The research in this thesis will also develop a permanent magnet movement in multilevel displacement while it also maintains minimum force as required.

2.9 Electric Current Regulator

Electric current regulator is a component or a group of components that is used to hold or adjust the value of electric current which flows in a circuit. There are some of possibilities in building an electric current regulator, such as by using voltage regulator or transistors. A voltage regulator (LM317) can be utilized to build a current regulator because of its characteristic which makes the voltage difference between its output pin and adjustment pin is always 1.25 volt when operated. In order to have certain value of electric current, as shown in Figure 2.18, a resistor is series connected between adjustment pin and output pin and to vary the value of flowing current, a variable resistor is connected as shown in Figure 2.19. So that the current can be calculated respectively:

$$I = \frac{1.25}{R} \text{ and } I_R = \left(\frac{1.25}{R}\right) \times \left(1 + \frac{R1}{R2}\right)$$

Figure 2.17

Voltage Regulator Based Fixed Current Regulator

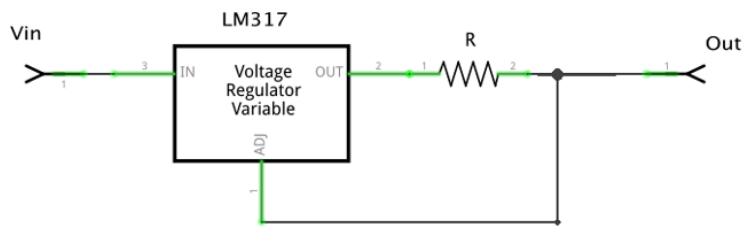
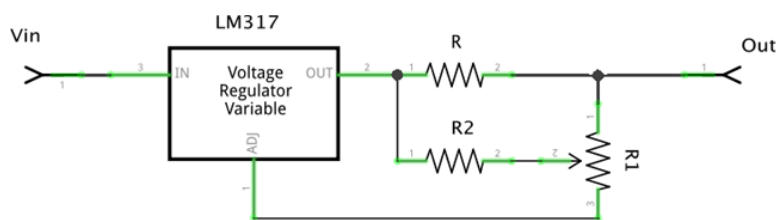


Figure 2.18

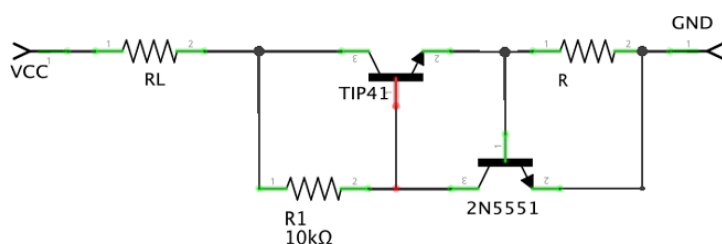
Voltage Regulator Based Variable Current Regulator



The other way to regulate the current is by applying transistors and shunt resistor. The circuit as shown in Figure 2.20 is placed after the load before the ground. The main components to build this circuit are power transistor (TIP41), control transistor (2N5551), and shunt resistor (R). The R_1 acts as a bias resistor. The working principle of this circuit is when the load resistance (R_L) become higher, the voltage drop across the shunt resistor will become higher as well. This condition triggers the control transistor to supply higher voltage at the base of the power transistor to let the current increased or reduced, so that the current supply will be kept stable. In order to vary the electric current using this circuit, a variable resistance can be added parallelly to bias resistor (R_1).

Figure 2.19

Transistors Based Current Regulator



2.10 Chapter Summary

The application of the technology in haptics becomes wider nowadays. Haptics technology helps and or enhance the process of information conveying. This goal achieved by using many kinds of actuator to result in different mechanisms. These mechanisms produce different sensation according to the information type which be delivered using certain method. The specific method to choose an option to build any actuating unit in haptics for information conveying usually depends on the speed of change which results in tactile sensation.

The needs in representing specific information using tactile sensations keep growing, especially for those with visual impairment. The role of haptics become greater and greater. Compact and portable devices would be great in helping visually impaired people. In other hand, for normal people, gaining information by experiencing multi-sensory effect is better than only to see it or hear it.

Electromagnetic actuator, especially functioned as solenoid, is one of the common actuators that is used in the haptics technology. The fast speed in response and the strong of the force produce by this type of actuator are the reason to use the electromagnetic. Because of the relation between the electric current and the produced magnetic force, the electric current must be driven to emit different value in magnetic force. Electric current regulator that can be controlled is needed in order to create the ability in producing variative magnetic force.

In this research, a haptics display board is developed. The working principle is like the BlindPad with pin variation enhancement. The electromagnetic actuator is occupied to produce up and down pin movement by vary electric current flows inside a pair of coils. Since the image processing grows very rapidly, a representation of a color in grayscale is able to be an input for this developed haptics display board.

CHAPTER 3

METHODOLOGY

The objective of this research is to create an electromagnetic-based haptic display that has the ability to adjust the height of each magnetic pin to stop at a certain point according to the data sent. In order to reach that goal, there are several steps taken. Detailed steps and calculations are written in this chapter. The designed circuit, hardware, and software, along with the realized one, are shown in each step explanation.

3.1 Working Step

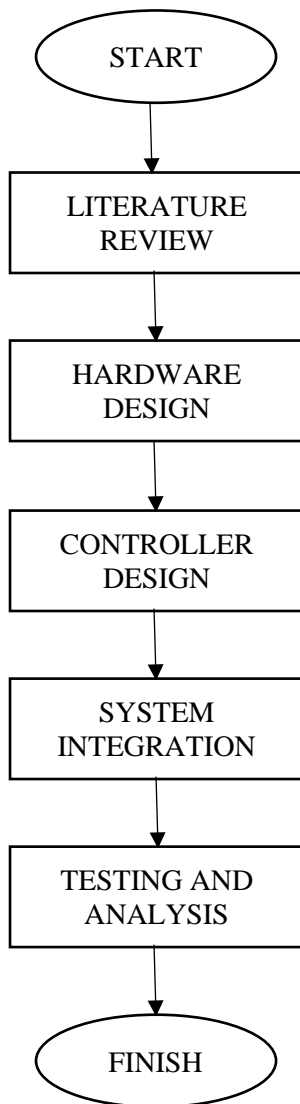
There are five main steps in this research, which are: literature review, hardware design, controller design, integration, and the last step for testing and analysis. The flow of the working step is shown in Figure 3.1. Some steps have its respective sub-steps to achieve the goal. Hardware designing is started by developing a single cell unit of a pin movement mechanism.

The literature study aims to obtain a sufficient basis for carrying out hardware designs, controller designs up to testing and analysis methods. Single unit magnetic pin movement, magnetic pins array, and the whole board for haptic display are the goals of the hardware design step. The controller design is a part where signal processing from the input and output signal on the actuator side is done. The joining between the hardware and controller side is implemented at the system integration process, followed by any needed testing and analysis to support the system working properly.

Electronic driver in controlling the flowing electric current utilizes the Metal Oxide Semiconductor Field Effect Transistor (MOSFET) that is explained in one part in this chapter about current regulator. The design of the full functioned hardware is divided into three steps, from hardware design to the system integration. Many experiments are conducted in hardware design steps, such as coil winding with different diameter of wire and the coil itself, dimension of the cells and permanent magnet along with the pins, digital data latching, and electric current regulating. Most of the parts of actuating unit are made by 3d printing and the driver by utilizing electronics components.

Figure 3.1

Working Step



3.2 Hardware Design

In order to achieve the final hardware that has a 3x3 board size, a single unit of the magnetic pin and a pair of coils is developed. This single moving unit is used to determine the size of each spot and the proper electronics component. Calculations and experiments are conducted in this step. Some details about the hardware are explained below.

3.2.1 Working Process of Haptics Display

Three main groups of components are implemented in the development of the haptics display, which are input, process, and output group. On the input group, there are an input instrument and the controller itself which shows an application on the screen, to

inform the desired value to the system. The values that have been inputted then will be processed programmatically by the controller. The illustration of the working process can be seen in Figure 3.2.

Figure 3.2

Working Process of The System



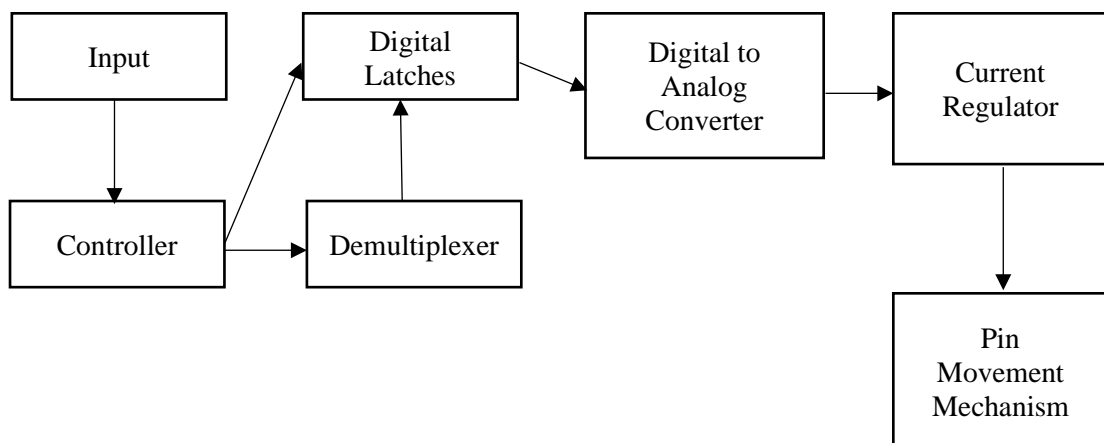
The controller also drives some support components in order to make the data flows inside the same lane alternately. The input is in the form of set of values that is entered to the system by using the Graphical User Interface (GUI) on the Raspberry Pi. The haptics display board includes the driver as well.

3.2.2 Block Diagram of The System

The pin's up and down movement is controlled by a driver. This driver consists of some main components, which are digital to analog converter and current regulator. The detailed part of the system is shown in the block diagram in Figure 3.3. The input is processed in the controller results in the digital bit to be sent to the driver.

Figure 3.3

Block Diagram of The System



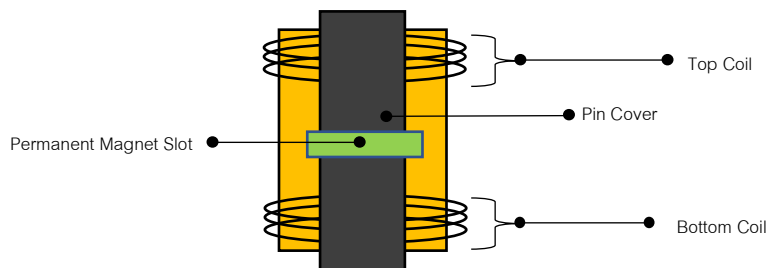
Since there are many pins to control, so the digital latches are enabled by the demultiplexer to send the bits to the driver alternately. This demultiplexer acts like a ring counter, is also driven by the controller to execute the flow of the bits at the set time and value. The current regulator is also equipped with the ability to transfer various voltages, based on the setting on the buck converter, as long it is needed to make the pin movement better and to achieve that the pin can withstand a certain load on it before it is stopped by the braking system.

3.2.3 Actuator Board Design

A pair of coils is controlled by a driver to move the magnetic pin inside. In order to obtain a precise specification of the coil, voltage, and current to be applied in moving the pin as desired, a single unit of pin movement mechanism is built. The principle of the mechanism is to vary the current flowing through the coil to obtain permanent magnet movement according to the digital value received from the controller. The parts of this single unit pin can be seen in Figure 3.4.

Figure 3.4

Single Unit of Pin Movement Mechanism



The top coil and bottom coil are synergized when they are energized to achieve a certain height of the permanent magnet covered by the pin cover. The pin cover is able to move up and down along with the permanent magnet. The up and down movement range of the pin cover top surface is 0 to 1cm. The movement is limited by the permanent magnet slot so that the whole pin will not pop up outside the case.

Enamelled copper wire (magnet wire) is used to build the coil winding, as shown in Figure 3.5. In order to fulfill the dimension of the board and the need for magnetic force related to the electric current flow, after some trials, 0.20mm outer diameter magnet wire was chosen. In American Wire Gauge (AWG), this copper wire is numbered 33.

Each coil has 250 turns, 6mm inner diameter, and 12mm outer diameter. The dimension of the coil was determined using the Brooks Coil approach.

Figure 3.5

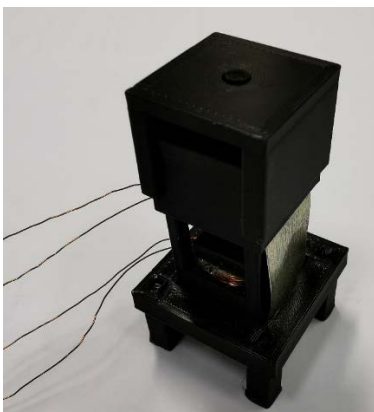
Coil Winding



In order to make the movement of the pin smoother without oscillation (swinging motion) a ferromagnetic sheet is added on the outside wall of the cell, as shown in Figure 3.6. This addition makes the single pin moves directly to the end point of the movement based on the amount of the electric current supplied in the coils. The ferromagnetic sheet helps to reduce the permanent magnet in one cell interfering with each other, since the magnetic force cannot be blocked but can be redirected.

Figure 3.6

Single Cell with Ferromagnetic Sheet Outside

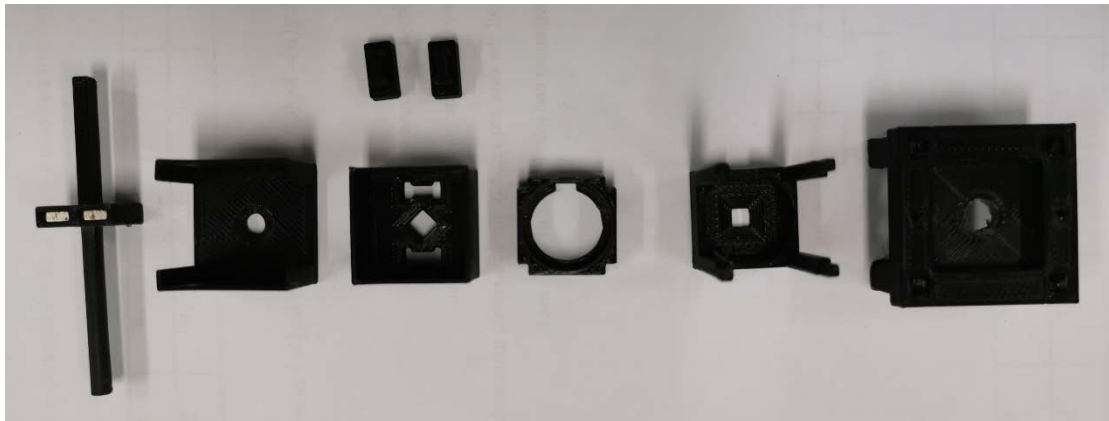


The single cell consists of two coil bases for the lower and upper coils, coils, pin rod with magnet slot, permanent magnet, base offset stand, top cap for the brake mechanism, and top cover (Figure 3.7.). The braking mechanism is needed since the

energized coil produces much heat when it is turned on for more than a second. The heat can melt the plastic parts of the cell. Most of the parts of the cells are made by 3D printing using polylactic acid (PLA) thermoplastic material, so that the high heat of the coil must be avoided. The braking system is built to address this high heat issue.

Figure 3.7

3D Printed Single Cell Parts

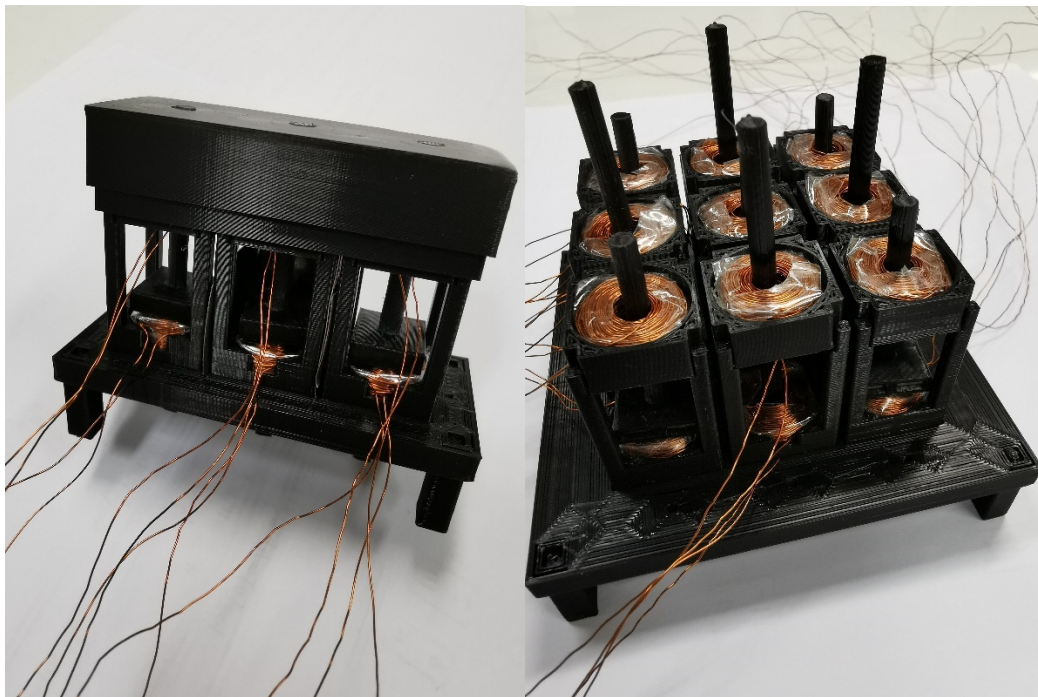


After making the single cell unit, the hardware-making process continued by simulating one row (three cells) and finally making the whole actuating board which consists of nine cells (Figure 3.8.). Some of the individual parts are printed together to become one part to build the nine cells board. The ferromagnetic sheet, to redirect the magnetic force and avoid the permanent magnet to interact each other, place a least on three outsides of each cell, except for the cell in the middle of the board. The cell in the middle has four walls made of ferromagnetic sheet.

The braking mechanism is made by printing a holed rod. The hole on this rod is layered by latex on a certain point in order to increase the friction between the rod and the pin, since the original friction among the 3D printed parts is too low. The shifting movement of the braking let the pin to be freed or locked. A servo motor is used to shift the rod. A rod is made for a row, so that for 3x3 dimension of the haptics display, three rods are occupied in the braking system.

Figure 3.8

Three and Nine Cells Actuating Board



A fishing line is used to connect the braking rod with the servo motor. The diameter of the fishing line is 0.6 mm. Two ends of each braking rod tied by the string and connected to motor. The angle rotation of the motor makes these rods shifting as acting in freeing and locking the pin. A pair of rail guides is added for each braking rod. This guide is important to make the latex layered side inside the rod's hole brushing the related pin. The brake mechanism can be seen in Figure 3.9.

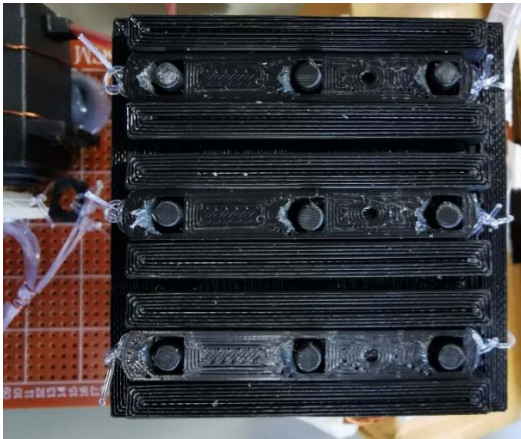
The addition of the braking mechanism makes the stopped pin at desired position can withstand certain load. The weighted loads which are some coins, are placed on the top surface of the pin. The weight of the stacked coins is 50 up to 75 gram. The pin's height is measured before and after the placement of the load on it. The pin's height is well maintained by the system, which means the braking mechanism can hold the pin's position even though there is a 75 gram load on the pin. This value of load's weight can be approximated in Newton which is ± 0.75 N.

The wire end on the final actuating board which consists of nine cells are put in order by labelling them and bind them on the one point to be connected to the driver through a breakout board. On this board, each end of the wires is soldered and connected into a

male pin. Female to female jumper cables is used to connect between the driver board and breakout board. The same cable is also used to connect between each part of the hardware block.

Figure 3.9

Brake Mechanism

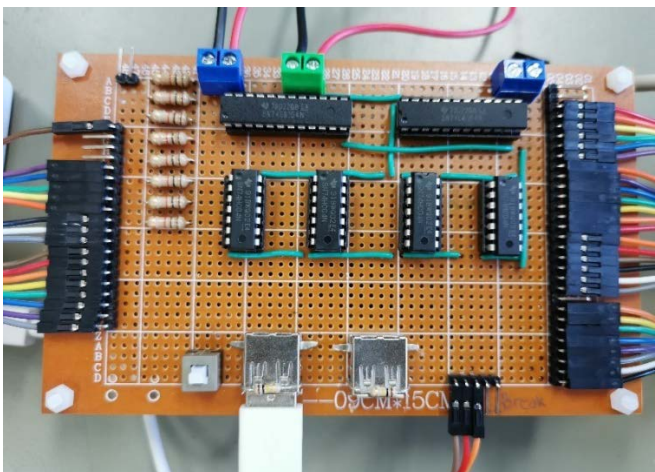


3.2.4 Bridge Board

The bridge board is a board connecting between the controller and the drivers. This board consists of some sockets for the power source and I/Os (Inputs and Outputs), switch button, and some ICs. The power input sockets receive the power from buck converter which is delivered to the controller, the board itself, servo motor, and the drivers. The details of this board are shown in Figure 3.10.

Figure 3.10

Bridge Board



The pinouts of the bridge board are divided into two parts which are input and output. The list of these pinouts is shown on Table 3.1 and Table 3.2 respectively. The numbering of the pins is counted from the top of the board. There are 20 input pins and 30 output pins provided by the bridge board. This board process the output from the controller to be distributed to the driver board.

There are two types of digital ICs installed on the bridge board. The first one is the demultiplexer IC (74154) which functioned as a driver selector. And the second one is not gate (7404) which functioned to invert the output from the demultiplexer since the inverting output is needed to control the load enable of the digital latch IC. A switch button is also on the board to totally cut off the power supply to the ports which are used to supply the power to the controller and display screen.

The data bit value from the controller is directly forwarded to the output pin. This data bit is sent to the all-digital latch IC but the data is executed to be shown alternatively by controlling the load enable pin on the digital latch IC. Additional set of pins on the bridge board is used as a connector to the servo motor, which are +5VDC, ground, and Pulse Width Modulation (PWM).

Table 3.1

Bridge Board Input List

Pin Number	Function	Pin Number	Function
1	Ground	11	Output Enable
2	Ground	12	PWM for servo motor
3	+5V (A)	13	Data bit 0 (LSB)
4	+5V (B)	14	Data bit 1
5	Selector bit 4 (MSB)	15	Data bit 2
6	Selector bit 3	16	Data bit 3
7	Selector bit 2	17	Data bit 4
8	Selector bit 1	18	Data bit 5
9	Selector bit 0 (LSB)	19	Data bit 6
10	Load Enable	20	Data bit 7 (MSB)

Table 3.2*Bridge Board Output List*

Pin Number	Function	Pin Number	Function
1	Ground	16	Load Enable 13
2	+5V	17	Load Enable 14
3	Load Enable 1	18	Load Enable 15
4	Load Enable 2	19	Load Enable 16
5	Load Enable 3	20	Load Enable 17
6	Load Enable 4	21	Load Enable 18
7	Load Enable 5	22	No connection
8	Load Enable 6	23	Data bit 0 (LSB)
9	Output Enable	24	Data bit 1
10	Load Enable 7	25	Data bit 2
11	Load Enable 8	26	Data bit 3
12	Load Enable 9	27	Data bit 4
13	Load Enable 10	28	Data bit 5
14	Load Enable 11	29	Data bit 6
15	Load Enable	30	Data bit 7 (MSB)

The power source for the controller is distributed by this board using a Universal Serial Bus (USB) socket. The additional USB socket is also provided for the display screen as long as needed. The provided voltage nominal on this USB socket is around +5.2VDC as the controller needs this value to keep its not in undervoltage condition. There are two buck converters from the battery toward this board, the first is for the ICs on this board and ICs on the driver boards, delivers +5VDC. And the second buck converter supplies the controller and for the display screen specially.

3.2.5 Digital to Analog Converter

Digital to Analog Converter (DAC) is the first part (Figure 3.11.) of the complete driver board (Figure 3.12). The voltage value is needed as an input for the driver to regulate the electric current flowing inside the coil. Since the output of the controller is in the digital form, another device is used to convert the controller's output into analog value.

The controller produces 8 bits digital value which means 0 to 255 in decimal. This set of values is delivered using a kind of bus connection to all of the digital latch buffer.

Integrated circuits named DAC0800 series (DAC0800 and DAC 0808) are used to do the conversion. One of the requirements of this circuit is to involve negative voltage as reference. The circuit is equipped with another battery supply to gain the negative voltage value. The nominal of the required negative voltage is -15VDC, this value is achieved by using a boost converter connected to the additional power source.

An additional set of values that consists of 5 bits digital value is sent to the bridge board to execute the digital latches alternatively. These 5 bits are functioned as a selector for the demultiplexer output, this mechanism acts as ring counter but with ability to change the output from high to low and vice versa. Selected lane on the demultiplexer delivers the load enable value which is regulated by the controller.

The digital value sent to the DAC must be hold in one data sending session. This because the digital lane is used in common with the other DACs. After certain value sent into specific pin number, digital latch is in charge to keep the same value until the next value is sent. An IC, digital IC 74573, acts as digital latch on one line of the driver, it means to drive one coil. The load enable pin makes it is possible to deliver the digital values alternatively among some digital latches.

Figure 3.11

Digital to Analog Converter Circuit



The wire connection from the controller to the driver is simplified by using a set of cables that is used to supply the data to all the needed components. The number of digital values to control one coil is eight bits. These bits are sent to all of the digital latches, but only one of them will keep these values at a time. This achieved by using the demultiplexer and five additional bits to create the sequence in executing the latching process.

Figure 3.12

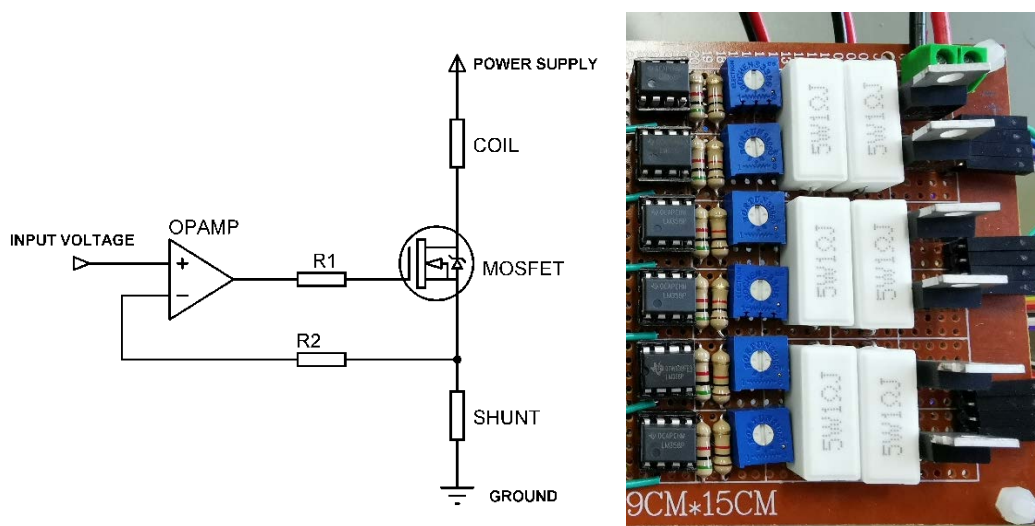
Driver Board



3.2.6 Voltage Controlled Current Regulator

Current regulator which is controlled by the voltage is the second part of the driver and the main part of the driver to control the actuator. The amount of magnetic force produced by electromagnetic coils depends on the electric current flowing in them. The digital output from the controller is converted to a voltage value by using a digital to analog converter. This produced voltage is used to regulate the flowing electric current in electromagnetic coils. The individual electromagnetic coil is driven by a voltage-controlled current circuit, shown in Figure 3.13.

Figure 3.13
Current Regulator Circuit



This circuit consists of an operational amplifier (op-amp), MOSFET, and some resistors. One of the rules used by op-amp to work is to make the difference between its two inputs; non-inverting and inverting input is always zero. The current regulator circuit utilizes an op-amp voltage follower connection. In the op-amp voltage follower circuit, the output of the op-amp is connected to the negative (inverting) input terminal, so that makes a 1x gain amplifier. Therefore, the voltage given across the input is available across the output.

The op-amp makes the differentiation of both inputs become zero (0). Because the output is connected across the inverting input terminal, the op-amp will produce the same voltage that is provided across the other input terminal. This happens for all negative feedback operations of an op-amp. The negative feedback in the current regulator circuit is derived from the shunt resistor connected across an N channel MOSFET instead of the output terminal of op-amp connected to the negative input terminal directly.

Any value of voltage given across the positive (non-inverting) input of the op-amp will make the op-amp produces a negative feedback path with the same value as the positive input at any cost. The output will turn on the MOSFET to get the same value as the input across the negative terminal. The role of the shunt resistor is to produce a drop voltage according to Ohm's Law that the voltage (V) is the multiplication between the

resistance (R) and the current (I). Therefore, the same value as input voltage drop will be produced if a specific current value flows through the shunt resistor. The value of the shunt resistor is fixed at a certain value so that the input voltage from the op-amp non-inverting terminal will vary the electric current value flowing through the shunt resistor.

The op-amp uses the drop voltage across the shunt resistor and gets the desired feedback. A load that requires current control for operation can be placed at an appropriate location, which is between positive terminal power source and drain pin of the MOSFET. Thus, the electric current through the load is equal to the electric current through the MOSFET which also equal to the current through the shunt resistor. Described mathematically as below:

$$\text{Current to the load} = \frac{\text{Voltage drop}}{\text{Shunt resistance}}$$

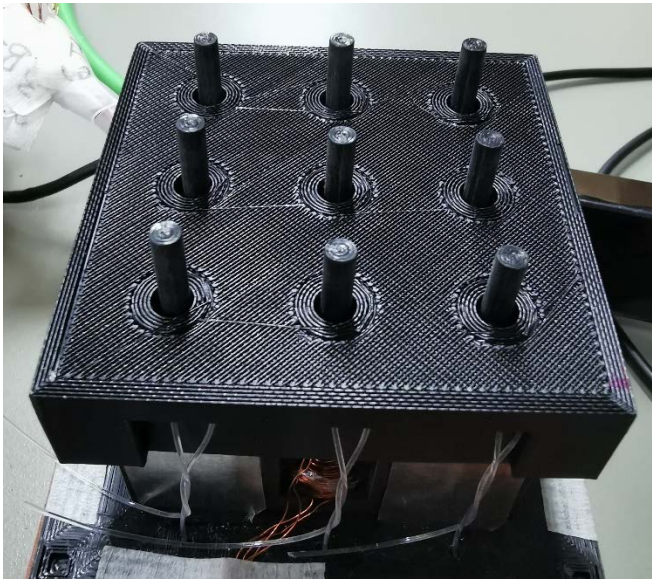
Voltage drop is the same as the input voltage across the op-amp. Therefore, if the input voltage is changed, the electric current through the load is changed as well. Hence,

$$\text{Current to the load} = \frac{\text{Input voltage}}{\text{Shunt resistance}}$$

In this research, the shunt resistance is fixed to one Ohm, however the output from the DAC circuit is regulated using precision potentiometer. The potentiometer is functioned to adjust the analog voltage value for each coil so that with the same digital value, equal height of the pin is produced for the related pin. This because of every coil are wound manually by hand, even though the number of turns is the same on all coils, there is still some slight differences in dimension.

Figure 3.14

Pins at Maximum Height



The limitation that is created by the potentiometer makes the range of the flowing current inside of a coil is between 0 and 1.8 Ampere. The supply voltage from the buck converter for the coil is 9VDC. On the other hand, the maximum power consumption when all of the 18 coils are powered using the highest current is around 580 watt for a short time before the locking process by the brake. However, the supplied electric current to the coils is always in the opposite proportion between the lower and upper coils, so that the maximum power consumption is about 300 watt for a short time when all of the pins are set at the highest point (Figure 3.14).

3.3 Controller Design

The system runs according to any set input sent to the driver. The controller is functioned to receive the input from the user and to process it so that the desired values are delivered respectively to each actuator through the driver. Some settings and mechanisms to control the actuator is provided by using simple programming code. Raspberry Pi is used to do the control function. A process sequence is executed every time the output updated.

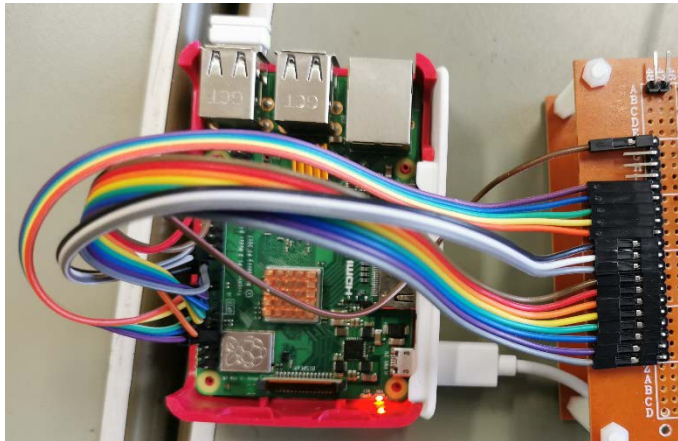
3.3.1 General Purpose Input/Output (GPIO)

An interface is used for communication between the controller, Raspberry Pi, with the hardware outside it. Raspberry Pi is equipped with a set of pins named General Purpose

Input/Output (GPIO). Raspberry Pi 3B has 40 GPIOs. These pins can be set as an input or an output, even can acts as PWM output to drive the servo motor. The Raspberry Pi board can be connected to a display screen by using HDMI connector or can be operated remotely using a computer.

Figure 3.15

Raspberry Pi GPIO



Digital output and binary number play their role to deliver the desired values to be actualized in regulating the electric current in the coil and trigger the driver to control the coil simultaneously. In order to fulfill these requirements, 14 digital out pins are utilized (Figure 3.15). The first 8 bits deliver a digital value of 0 to 255 to be converted to analog signal as a voltage. The second 5 bits send the binary value to the demultiplexer so that the selected lane will be activated to convey the data to the desired driver circuit to control a certain coil. The last bit is used to create a clock signal to trigger the buffer to continue data flowing in it to the output. The list of the use of the GPIO is shown in Table 3.3.

Table 3.3*Raspberry Pi GPIO List*

Pin Number	Function	Pin Number	Function
33	Data bit 0 (LSB)	18	Selector bit 0 (LSB)
37	Data bit 1	16	Selector bit 1
7	Data bit 2	12	Selector bit 2
11	Data bit 3	10	Selector bit 3
13	Data bit 4	8	Selector bit 4
15	Data bit 5	22	Load Enable
19	Data bit 6	24	Output Enable
21	Data bit 7 (MSB)	26	PWM for servo motor

The process sequence starts with the initial set up by making all of the digital value for the coils set to zero and the brake is on the active position. The main process of the digital values delivery to the driver is the look up process from a reference file and recalculate the pre delivered value. This reference file is made manually by sending and measuring a certain value to the actuating unit. This calibration process is done by tuning the potentiometer on each driver to gain the maximum pin height position.

The values, which are processed by the system, are stored in an array. The members of the array are used to do the calculation process and gain the decimal values that are sent to each driver and power up the corresponding coil with certain amount of electric current. The array, either in millimeter or decimal value is the gate to create a possibility to connect the developed system with the additional system such as image processing unit. The addition of the number of the pins must be accompanied by the expansion of the driver and the selector bits.

Completed initiation process is followed by the deactivation of the brake, it means the pins are freely to move up and down. A certain value from the input makes the system looks for the nearest reference point above and below the desired value and then calculate the values that should be delivered to the coils. The suitable values for a pair of coils are acquired after the processing the reference value from the file. The cycle of sending the values begin from here.

Since there are nine pins on the board, 18 values need to be sent to the driver. The coils are numbered from 1 to 18, in example lower coil of pin number two is number three, the upper coil of pin number two is number four, and so on. Mention the value for the third coil is A and B for the fourth coil. At a time, the bus which sends the data bits to the driver is carrying the A value in parallel with the selector value is three. Selector bit makes the demultiplexer let the load enable value pass the output number three and trigger the digital latch IC to forward and hold the data bits to its output.

Values held successfully on the third digital latch is then followed by the next process which disable the load enable pin on the corresponding digital latch. The A value remains on the third latch IC and the bus carries the next value which is B. The selector, enable, and disable process is repeated. These processes occur until the last value is sent to the driver. The brake mechanism locks the pins as soon as possible after the last data bits sent to the driver.

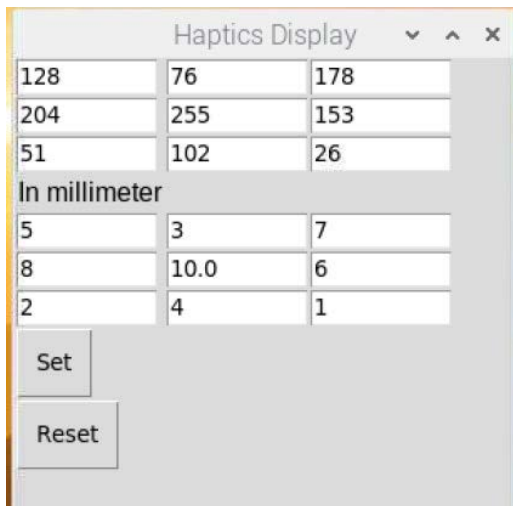
Locked pins do not need the magnetic force from the coils anymore. So that the coils can be deactivated in order to save the energy and to avoid the excessive heat that makes the plastic parts of the cell bend or melt. Initiation process is triggered again after the pins are locked. The load enable value is set to high since the needed value is low and the selector is set to zero which means no active lane for the load enable on the demultiplexer. The sequence process for a set of values is completed on this point.

3.3.2 Graphical User Interface (GUI)

Graphical User Interface is built using Python on Raspberry Pi to ease the input of the value to the board. This process utilizes the GUIzero library to create interactive display and input to the user. As shown in Figure 3.16, the GUI consists of several text boxes to input the values in decimal (0-255) or in millimeter (0.0 – 10.0) and two buttons which are set and reset.

Figure 3.16

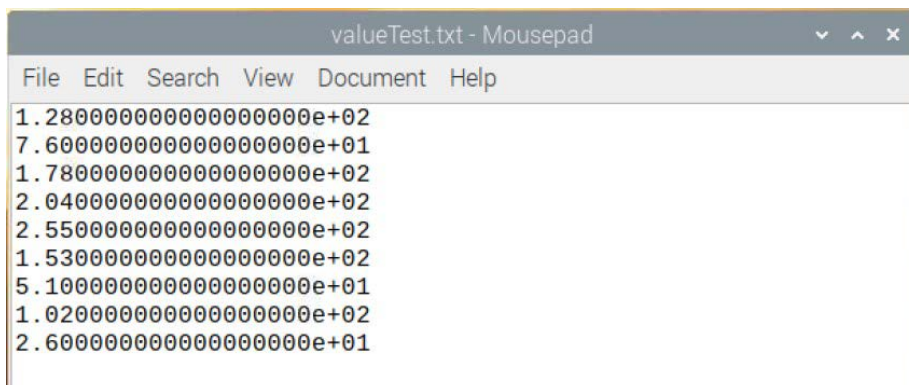
Graphical User Interface



The loading process of the application opens last saved pins height values in a file. These values are inputted in the text boxes on the form. The set button is used to start the sequence in setting the pins height on the actuating board. Pressed set button also saves the values on the text boxes into a text file whenever any change occurs on the text boxes and the set button is pressed. This file is used to load the data when the application is started. The sample of the file that stores the last set values is shown in Figure 3.17.

Figure 3.17

Last Recent Values File



The change in a certain text box, as an event, calls a function to update the corresponding text box, the pair of the text box. The value which is inputted in decimal makes the value in millimeter directly updated based on the recent decimal value and

vice versa. The group of values which is processed by the system is the values in millimeters. These values fill an array and the members of this array are used to determine the decimal value for each coil.

Reset button is used to makes the pin position on the maximum below point. On the other hand, reset button starts the process in setting all of the upper coils in its maximum value. The maximum value is set to 200 in decimal and the voltage which controls the MOSFET in passing the certain electric current amount is limited by turning the potentiometer. In short, the reset processes are freeing all of the pins by deactivating the brake, set all of the upper coils in its highest value, activate the brake, and finally execute the initiation cycle to make all of the coil's values become zero.

3.4 System Integration

The hardware consists of four separated modular parts, starts from the controller, bridge board, actuator drivers, and the actuator board itself. The wires of the actuating board have a breakout board to ease the connection to the driver board. Each connection between parts is using female to female jumper cables. The bigger diameter of cables is used to supply the power from the battery to the Direct Current (DC) to DC converter and from the converter to the related board.

Connection of all the modular boards is followed by testing the output of the Digital to Analog Converter circuit in order to make sure that the analog values are ready to be used to drive the current regulator. Different values in the form of the 8 bits data are set for each driver to prove that the data bus and selection process work properly. The actuating board is connected after the testing results the optimum condition as designed.

The rod of the brake is connected to the motor by a string. The angle of the servo motor is set to 90 before the two ends of the string are connected on it. The purpose is that the motor can be adjusted whether clockwise (CW) or counter clockwise (CCW) to gain the optimum position in locking and freeing the pins. An experiment is done to obtain the exact angle value either when pins are locked or freed. This process is important to support the measurement process in order to maintain the height position remains the same at a time.

The system is ready to supply the power to the coil. In order to vary the pins height by differing the flowing electric current, a reference file is needed. This file is loaded by

the system as an array that is used to calculate the decimal value to be sent in the form of 8 data bits to the driver board. Measurement of the height of the pin is done by using a digital caliper (Figure 3.18). The first position to store is the maximum position of all the pins. The initial decimal value is 200 which points 1.8 Ampere on the driver board. The purpose of choosing this value is that the decimal value can be adjusted up and down along with the potentiometer. Since turning the potentiometer cannot result in light difference of the amount of the pins height.

The response time of the system is calculated by summing the needed time from the set button is pressed until the system finishes the process sequence in setting the pin's position. The processing of the interpolation calculation and array filling by the controller is assumed to be held in 0.2 second. This approximation is taken by observe the running script and the number of the lines of the script. Besides, there are some time delays in executing the braking mechanism for the deactivation and activation of the brake for 0.6 second. In summary, the total response time of the system in processing the input and showing the desired output is 800ms (0.8 second).

Figure 3.18

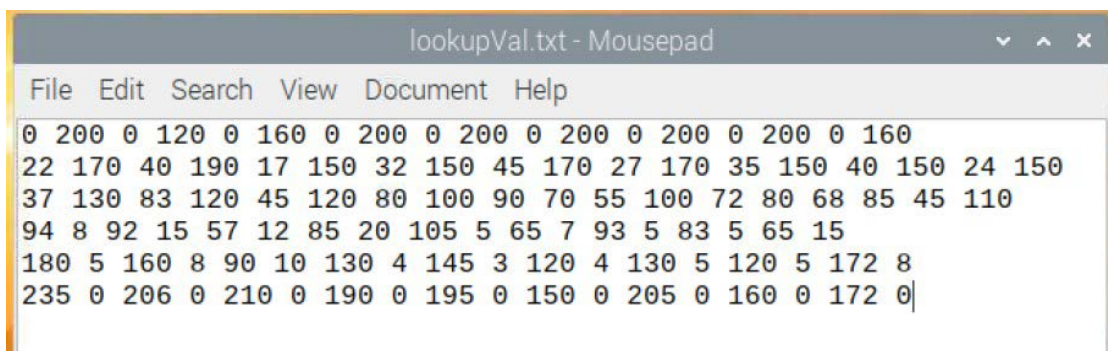
Measurement Process



Every single pin is measured and the decimal value in gaining certain position is noted and stored in a text file. The format of this reference file is grouped row by row where each row represents same height value of all pins. Each row consists of 18 decimal numbers since there 18 coils for nine pins. On the other hand, there are 9 pairs of decimal values in a row. The specific number is called by the system in the form of an array. Recalculation is done as long as needed if the desired value is not exactly on the reference list. The sample of the reference file can be seen in Figure 3.19.

Figure 3.19

Text File of Reference Values



3.5 Chapter Summary

The main process in developing the hardware is the system integration among all of the parts. Three main groups of the hardware which are input, process, and output were connected and result in haptics display system. The system works by varying the amount of the electric current flowing inside the coils. This electric current variation produces different magnetic force that lifts certain pin in different height. The pins are locked while they are at the desired position as set by the input. This locking process makes the board can be groped and deliver the tactile sensation that can be used to deliver certain information especially for the people with visual impairment.

The process of designing and making process of the hardware were discussed in this chapter. The hardware is able to vary the pins height according to the reference values that are stored in a text file. The process in sending and set all of the pin's height occurs for less than a second. Even though, every single sequence needs to make all of the pins back to their maximum below position (minimum position). Testing process is needed to confirm and fulfill the proposed requirement.

CHAPTER 4

RESULTS AND DISCUSSION

System integration which integrates the controller, bridge board, drivers and actuator; needs to be tested. Some tests are done and reported in this chapter, especially in fulfilling the proposed design. The system repeatability and accuracy are the main points to be measured and discussed in this chapter. Some experiment results are averaged to mention the performance of the system.

4.1 Repeatability

The system is set to output a certain value and this command is repeated several times to observe the result. The variation of the results is compared each other. The fewer result variation compared to the average of the results means the system repeatability is good. The difference between the values with the average one is the error. The repeatability is stated standard deviation value. The experiments are conducted for several input command to obtain the general repeatability of the system without any calibration before the experiment, since this experiment aims to observe the comparison among the measured value.

There are four measurements in observing the height of the pin. Each measurement results in different range of height. Starts from the lowest range to the highest one. The Standard Deviation (SD) from each pin in each observation is calculated and every test produces Pooled Standard Deviation (PSD) which is the average from standard deviation form each pin. The good repeatability is achieved when the final standard deviation as near as possible with zero value. The formula to determine the PSD value:

$$\text{PSD} = \frac{\text{SD}_1^2 + \text{SD}_2^2 + \dots + \text{SD}_k^2}{k}$$

where k is the number of the data population, in this case the number of pins which is 9. The result is stated with 3 digits decimal value (three digits behind the comma).

Relative Standard Deviation (RSD) is also shown as indicator to see the spread of the data from the mean of the results. This value is also written in percentage to ease of understanding. The good repeatability is indicated by the small RSD value, as near to zero value. The RSDs from each pin are used to determine the Pooled Relative Standard Deviation (PRSD), as well as in percentage value, to state the RSD of single test. The formula to calculate RSD and PRSD value are:

$$RSD = \frac{SD}{x_{mean}}$$

$$PRSD = \frac{RSD_1^2 + RSD_2^2 + \dots + RSD_k^2}{k}$$

where x_{mean} is the average value of the measured height of certain pin and k is the number of data population, in this case is the number of the pins which is 9.

The first measurement for the repeatability test is done with the range of the pin's height from 3 to 7 mm. The results are shown in Table 4.1 and 4.2.

Table 4.1

First Repeatability Test Result

Pin Number	Set Point (mm)	Measurement (mm)									
		1	2	3	4	5	6	7	8	9	10
1	7	6.91	6.99	7.14	7.14	7.19	7.22	7.20	7.20	6.93	7.14
2	3	3.64	3.58	3.60	3.59	3.43	3.52	3.55	3.48	3.44	3.41
3	6	5.63	5.52	5.44	5.55	5.58	5.58	5.62	5.58	5.64	5.61
4	4	4.52	4.35	4.50	4.56	4.47	4.46	4.52	4.73	4.45	4.52
5	4	3.87	3.53	3.77	3.93	3.57	3.58	3.77	3.69	3.76	3.74
6	6	5.88	5.83	5.72	5.95	5.92	5.75	5.75	5.72	5.90	5.84
7	3	3.48	3.50	3.48	3.52	3.51	3.52	3.51	3.51	3.51	3.52
8	5	5.01	5.10	4.97	5.08	5.07	5.03	5.01	5.08	5.04	5.04
9	7	6.79	6.68	6.67	6.83	6.82	6.75	6.56	6.75	6.83	6.79

Table 4.2*Standard Deviation of First Test*

Item	Pin Number								
	1	2	3	4	5	6	7	8	9
Set Point (mm)	7	3	6	4	4	6	3	5	7
Mean (mm)	7.08	3.54	5.58	4.5	3.72	5.83	3.5	5.05	6.75
SD	0.124	0.081	0.059	0.099	0.139	0.079	0.016	0.041	0.082
RSD	0.02	0.02	0.01	0.02	0.04	0.01	0	0.01	0.01
RSD %	2%	2%	1%	2%	4%	1%	0%	1%	1%
PSD	0.088								
PRSD	0.02								
PRSD %	2%								

The second measurement for the repeatability test is done with the range of the pin's height from 6 to 9 mm. The results are shown in Table 4.3 and 4.4.

Table 4.3*Second Repeatability Test Result*

Pin Number	Set Point (mm)	Measurement (mm)									
		1	2	3	4	5	6	7	8	9	10
1	8	8.35	8.33	8.56	8.25	8.63	8.20	8.44	8.40	8.53	8.56
2	6	6.36	6.37	6.36	6.34	6.40	6.34	6.41	6.44	6.37	6.44
3	7	7.32	7.45	7.43	7.33	7.28	7.61	7.70	7.78	7.60	7.65
4	6	6.34	6.42	6.66	6.32	6.34	6.32	6.47	6.46	6.43	6.51
5	6	6.05	6.01	5.94	5.73	5.94	5.84	5.83	5.91	5.75	6.08
6	8	7.76	7.90	7.78	7.75	7.75	7.92	7.71	7.87	7.86	7.79
7	7	6.57	6.59	6.54	6.61	6.67	6.73	6.58	6.75	6.67	6.61
8	7	7.45	7.40	7.41	7.47	7.42	7.26	7.42	7.37	7.52	7.56
9	9	9.11	9.02	9.04	9.09	9.10	8.88	9.08	9.12	9.15	9.12

Table 4.4*Standard Deviation of Second Test*

Item	Pin Number								
	1	2	3	4	5	6	7	8	9
Set Point (mm)	8	6	7	6	6	8	7	7	9
Mean (mm)	8.43	6.38	7.52	6.43	5.91	7.81	6.63	7.43	9.07
SD	0.144	0.037	0.176	0.107	0.12	0.072	0.07	0.082	0.077
RSD	0.02	0.01	0.02	0.02	0.02	0.01	0.01	0.01	0.01
RSD %	2%	1%	2%	2%	2%	1%	1%	1%	1%
PSD					0.106				
PRSD					0.015				
PRSD %					1.5%				

The third measurement for the repeatability test is done with the range of the pin's height from 7 to 10 mm. The results are shown in Table 4.5 and 4.6.

Table 4.5*Repeatability Third Test Result*

Pin Number	Set Point (mm)	Measurement (mm)									
		1	2	3	4	5	6	7	8	9	10
1	9	9.38	9.51	9.27	9.34	9.34	9.29	9.14	9.37	9.39	9.44
2	7	6.87	6.64	6.74	6.83	6.76	6.72	6.77	6.66	6.79	6.82
3	9	8.56	8.55	8.55	8.66	8.63	8.65	8.76	8.77	8.76	8.71
4	8	7.92	7.52	7.62	7.53	7.65	7.62	7.61	7.67	7.65	7.63
5	7	7.34	7.36	7.32	7.40	7.40	7.31	7.31	7.49	7.36	7.42
6	9	9.08	9.05	9.06	9.07	9.00	9.02	8.73	8.93	9.13	9.16
7	8	8.23	8.25	8.55	8.48	8.47	8.47	8.64	8.80	8.37	8.50
8	10	9.75	9.74	9.67	9.87	9.75	9.78	9.95	10.01	9.83	9.91
9	10	10.2	10.2	10.2	10.3	10.2	10.3	10.4	10.4	10.3	10.4

Table 4.6*Standard Deviation of Third Test*

Item	Pin Number								
	1	2	3	4	5	6	7	8	9
Set Point (mm)	9	7	9	8	7	9	8	10	10
Mean (mm)	9.35	6.76	8.66	7.64	7.37	9.02	8.48	9.83	10.29
SD	0.1	0.073	0.088	0.109	0.057	0.121	0.17	0.107	0.088
RSD	0.01	0.01	0.01	0.01	0.01	0.01	0.02	0.01	0.01
RSD %	1%	1%	1%	1%	1%	1%	2%	1%	1%
PSD					0.106				
PRSD					0.012				
PRSD %					1.2%				

The fourth measurement for the repeatability test is done with the range of the pin's height from 9 to 11 mm. The results are shown in Table 4.7 and 4.8.

Table 4.7*Repeatability Fourth Test Result*

Pin Number	Set Point (mm)	Measurement (mm)									
		1	2	3	4	5	6	7	8	9	10
1	9	9.32	9.31	9.44	9.48	9.46	9.27	9.39	9.43	9.49	9.41
2	10	9.82	9.72	9.54	9.83	9.70	9.64	9.89	9.64	9.60	9.56
3	10	9.93	9.90	9.84	9.79	9.82	9.82	9.84	9.84	9.79	9.78
4	9	9.07	8.91	8.93	8.96	9.11	9.03	9.11	9.02	9.10	8.90
5	9	9.03	8.95	9.08	8.94	9.00	9.10	9.03	9.11	8.95	9.04
6	9	9.33	9.61	9.66	9.43	9.53	9.68	9.73	9.61	9.49	9.36
7	10	9.73	9.66	9.74	9.76	9.73	9.77	9.72	9.68	9.72	9.69
8	10	10.1	10.4	10.4	10.3	10.2	10.3	10.1	10.1	10.1	10.1
9	10	10.5	10.4	10.5	10.7	10.5	10.5	10.3	10.4	10.5	10.5

Table 4.8*Standard Deviation of Fourth Test*

Item	Pin Number								
	1	2	3	4	5	6	7	8	9
Set Point (mm)	9	10	10	9	9	9	10	10	10
Mean (mm)	9.4	9.69	9.84	9.01	9.02	9.54	9.72	10.21	10.48
SD	0.076	0.12	0.048	0.084	0.063	0.138	0.035	0.129	0.103
RSD	0.01	0.01	0	0.01	0.01	0.01	0	0.01	0.01
RSD %	1%	1%	0%	1%	1%	1%	0%	1%	1%
PSD	0.095								
PRSD	0.01								
PRSD %	1%								

The repeatability of the system is stated by using the highest number for the PSD and PRSD to indicate the biggest data spread from the average measurement result. The general result of the repeatability test is the value of the PSD 0.106 and PRSD 2%. These values indicate that the system has the good repeatability since the standard deviation value and the relative standard deviation value are small.

The factors that affect the system performance for the repeatability are the friction between the pin and along the path that passed by the pin and the magnetic force produced by the pair of coils on each cell. Each pin with the permanent magnets inside the magnet slot has certain weight, and by applying the same input command which results in the same output magnetic force, makes the variation of the pins height is small.

4.2 Accuracy

The value from the measuring tool, in this case the digital caliper, is compared to the input value of the system to get the accuracy of the actuating board. Certain value is set as the input to observe the output. The closer output value with the input value means the accuracy of the system is good. The difference between the measurement result and the input value is the error. The accuracy is stated in percentage in each experiment. The experiments are conducted in several condition to obtain the general accuracy of the system.

4.2.1 Accuracy of Reference Value

Some values in the system are set by using a reference file. These values named reference value. The file contains six rows which saves decimal values to each coil for six different positions. The positions that are saved in the file are 0, 2, 4, 6, 8, and 10mm. This set of values is used to calculate the other input value. The measurement result is shown in the Table 4.9.

Table 4.9

Accuracy of Reference Value Test Result

Set Point (mm)	Pin Number									E	A
	1	2	3	4	5	6	7	8	9		
2	1.88	1.99	3.12	1.66	2.19	1.64	2.50	2.04	2.06	15	85
4	3.30	3.20	3.90	3.90	3.97	3.46	3.93	4.15	3.92	7	93
6	5.63	5.93	6.34	4.94	5.16	5.53	5.75	5.68	5.95	7	93
8	7.99	8.59	8.52	7.04	7.78	7.68	7.32	7.63	7.71	6	94
10	9.65	9.78	10.09	10.32	10.25	10.21	9.73	10.30	9.83	2	98

E = Error (%); A = Accuracy (%)

The error value is taken by calculate the different between the set point and the actual point divided by the input value. The error from every measurement is used to gain the average value of the error. The accuracy percentage is the number result of the subtraction from 100% by the average error value.

The lower value gives lower accuracy as per measurement result. The possibility factor that causes this to occur is the interaction among the permanent magnet on the initial position and the similar measured different which divided with the set point value. The general error for this first test average is 7% which means the accuracy can be concluded 93% in average for the reference value.

4.2.2 Accuracy of Estimated Value

The value outside the reference value is calculated based on the upper and lower value of the input value, named estimated value. This is can be integer of non-integer value, but in this experiment, all of the tested values are in integer since the non-integer value does not make significant tactile sensation feeling when the pins are groped. The result of this second accuracy test can be seen in Table 4.10.

Table 4.10*Accuracy of Estimated Value Test Result*

Set Point (mm)	Pin Number									E	A
	1	2	3	4	5	6	7	8	9		
1	0.82	0.85	0.73	0.98	1.36	0.87	0.88	1.44	0.48	24	76
3	3.06	2.76	3.45	2.54	2.94	2.90	2.74	3.14	2.96	7	93
5	4.75	4.35	4.71	4.56	4.70	4.29	4.59	4.91	4.72	8	92
7	6.61	6.75	7.47	6.14	6.32	6.65	7.11	7.06	7.09	5	95
9	8.47	9.08	8.33	8.57	8.41	8.94	8.86	9.60	9.07	4	96

E = Error (%); A = Accuracy (%)

As the previous measurement, the lower estimated value gives the lower accuracy. The range of the difference between the actual value with the set point is similar among the tested estimated value. In general, the error average of the estimated value is 10% which mean the accuracy result from this second test in average is 90%.

4.2.3 Accuracy of Combined Reference Value

In this third accuracy test, several reference values are combined to create different pin height at the same time. This is the main function of the board when it is operated to show or send the information.

Table 4.11*Accuracy of Combined Reference Value*

Set Point (mm)	Pin Number									E	A
	1	2	3	4	5	6	7	8	9		
2	-	-	2.56	-	-	-	2.08	-	-	4	96
4	-	-	-	4.22	-	3.98	-	-	-	1	99
6	-	5.64	-	-	-	-	-	6.17	-	1	99
8	7.97	-	-	-	-	-	-	-	7.19	1	99
10	-	-	-	-	9.34	-	-	-	-	1	99

E = Error (%); A = Accuracy (%)

The lower value results in lower accuracy as before, but the overall performance when the different values are sent to the actuating unit, the response is good. This because of

the calibration process meets very close to the set point. The biggest difference happens on the pin number five, because pin number five is the one and only pin in this prototype that has four ferromagnetic walls and surround by for other permanent magnets. This shows that the interference still occurs even though each cell is separated using the ferromagnetic sheet.

4.2.4 Accuracy of Combine Estimated Value

The last test for the accuracy measures the combined estimated values. This aims to check the functionality of the system in showing different pin height for the estimated value processed by the system. The result of the test can be seen in Table 4.12.

Table 4.12

Accuracy of Combined Estimated Value

Set Point (mm)	Pin Number									E	A
	1	2	3	4	5	6	7	8	9		
1	-	-	-	1.09	-	0.63	-	-	-	5	95
3	3.13	-	-	-	-	-	-	-	3.03	1	99
5	-	4.15	-	-	-	-	-	4.65	-	3	97
7	-	-	7.08	-	-	-	6.48	-	-	1	99
9	-	-	-	-	8.27	-	-	-	-	1	99

E = Error (%); A = Accuracy (%)

The ability of the system to output the combination of estimated value is good. The result difference from the set point is less than 0.8mm. The lower value shows lower accuracy as all of the previous tests. The performance of the system in this test in average is more or less 98%.

4.3 Chapter Summary

The difference between the setpoint and measured value in the repeatability test seems systematic error. This error happens because, in the repeatability test, the system is not calibrated yet. The repeatability test tests the system to produce the exact position of the same command in every measurement. After the calibration process, the error becomes a random error in the accuracy test. The difference among coil windings is the main factor that affects this error. The second factor is the hardware and software calibration tool cannot precisely give the exact value for the coil to achieve exact point.

The result of the testing process indicates that the system works as proposed designed. The general repeatability of the system is stated with the highest Pooled Standard Deviation value which is 0.106 and the Pooled Relative Standard Deviation which is 2%. These values show that the repeatability of the system is good. The accuracy that taken from the overall tests shows that in general the system has 95% accuracy in average. The lowest accuracy test result is used to determine the overall system accuracy which is 76%.

CHAPTER 5

FUTURE WORK AND RECOMMENDATION

The main purpose of this thesis is to make a haptics display prototype using an electromagnetic principle in changing the height of the pin on the board. The design step up to the realization results in a 3x3 haptics display board with the distance between the pins is 14mm. This distance is affected by the dimension of the coil. Since the coil was made manually by hand, the density might as good as expected. Special tool and machine are needed to produce the better coil density and dimension so that the used energy can be made more effective and the distance between the pins can be reduced.

Most of the parts of the display cell are made of plastic filament by 3D printing process. The material used is Polylactic Acid (PLA). In order to increase the heat resistance of the material, further experiment should be held. All of the parts which are in touch or in interaction with the coil must be solid enough to withstand heat for a certain time. The purpose is to maintain the original designed form, especially the pins with the permanent magnet slot.

The control is able to handle any input in the form of an array of values. This input can be gotten from an image processing software or similar application that needs to be represented using the variation of the pin's height on the board. A fusion or a blend of this developed device with additional system as an input can be done in order to expand the use of the haptics display board.

The expansion of the size of the board will be able to deliver more information variation. In this case, additional cooling system, such as a fan, should be use and place below the board. This fan is functioned to bring out the heat produced by the coil. In other words, bigger system size needs better exhaust system to send out the heat.

The other expansion possibility is to create additional system in supporting the calibration process. The energized coil can hold certain electric current for a moment by using better cooling system. In this case, sensor-based calibration tool can be added while the output value delivered to the coil varied to achieve certain height.

In the use of energy, the setting of individual pin will save much energy if it is done one by one. This needs the individual braking mechanism as well. The setting and braking mechanism can be set to at least row by row or column by column depends on the available input output pins that can be occupied. Better coil combined with smaller group activation will result in energy saving, since the drawback of this mechanism is the use of high power to activate all of the coils at the same time.

REFERENCES

- Akash Yadav (2016). Ferromagnetic Material for Strong Magnetic Shielding. The ICFAI University Dehradun, Dehradun, India.
- Ali Mousavi, Alireza Akbarzadeh, Morteza Shariatee, Salman Alimardani (2015). Repeatability Analysis of a SCARA Robot with Planetary Gearbox. Ferdowsi University of Mashhad, Mashhad, Iran.
- Cheng Xu, Ali Israr, Ivan Poupyrev, Et. al. (2011). Tactile Display for the Visually Impaired Using TeslaTouch. Disney Research Pittsburgh, Pennsylvania, USA.
- Ching-Chuan Su (2006). Mechanisms for the Longitudinal Recoil Force in Railguns Based on the Lorentz Force Law. National Tsinghua University, Hsinchu, Taiwan.
- Chris Deziel (2018). How to Calculate Percent Accuracy. Sciencing by Leaf Group, Santa Monica, California, USA.
<https://sciencing.com/calculate-percent-accuracy-6199228.html>
- Christopher R. Wagner, S. J. Lederman, Robert D. Howe (2002). A Tactile Shape Display Using RC Servomotors. Harvard University, Cambridge, Massachusetts, USA.
- Craig Shultz (2020), "Surface Haptics Technology Enriches Touchscreen Interactions", Haptic Experience Team, Tanvas, Chicago, USA.
- Felix G. Hamza-Lup, Kyle Bergeron, Daniel Newton (2019). Haptic Systems in User Interfaces - State of the Art Survey. ACM Southeast Conference, Kennesaw, GA, USA.
- Francine Gemperle, Nathan Ota, Dan Siewiorek (2001). Design of a Wearable Tactile Display. Carnegie Mellon University, Pittsburgh, USA.
- G. A. Belov, S. V. Abramov, G. V. Malinin, A. V. Salov (2019). Control Unit for Electromagnet Current. I. N. Ulyanov Chuvash State University, Cheboksary, Russia.
- Giuseppe Giuliani (2000). On electromagnetic induction. Dipartimento di Fisica 'Volta', Via Bassi 6, 27100 Pavia, Italy.
- H. R. Choi, S. W. Lee', K. M. Jung, Et. al. (2004). Tactile Display as a Braille Display for the Visually Disabled. Sungkyunkwan University, Suwon, South Korea.
- Harry Mafukidze (2021). How to Use Servos on the Raspberry Pi. Circuit Basics.

<https://www.circuitbasics.com/how-to-use-servos-on-the-raspberry-pi/>

- Hyun-A Ahn, Seong-Kwan Hong, Oh-Kyong Kwon (2016). A Fast Switching Current Regulator Using Slewing Time Reduction Method for High Dimming Ratio of LED Backlight Drivers. Hanyang University, Seoul, South Korea.
- Ing-Yann Albert Wang, Ilene Busch-Vishniac (1994). A New Repulsive Magnetic Levitation Approach Using Permanent Magnets and Air-Core Electromagnets. University of Texas, Austin, Texas.
- Jean-François BRETHER (2010). Intrinsic Repeatability: a new index for repeatability characterization. Le Havre University, Le Havre, France.
- Jerome T. Tzeng (2004). Structural Mechanics for Electromagnetic Rail Guns. U.S. Army Research Laboratory, Weapons and Materials Research Directorate, Aberdeen Proving Ground, USA.
- Jonatan Martinez, Adam Harwood, Hannah Limerick, Rory Clark, Orestis Georgiou (2019), “Mid-Air Haptic Algorithms for Rendering 3D Shapes”, Ultrahaptics Ltd., The West Wing, Glass Wharf, Bristol, BS2 0EL, UK.
- Jun Rekimoto (2014). Ambient touch: Designing tactile interfaces for handheld devices. University of Tokyo, Tokyo, Japan.
- Kunihisa Tashiro (2006). Broadband Air-Core Brooks-Coil Induction Magnetometer. Kyushu University, Fukuoka, Japan.
- Luca Brayda (2017). Personal Assistive Device for BLIND and Visually Impaired People. Project Final Report, Fondazione Istituto Italiano di Tecnologia.
- Mark S. Conradi, Hilary T. Fabich (2020). Precision current regulator for NMR electromagnets. ABQMR, Inc., Albuquerque, USA.
- Masami Shinohara, Yutaka Shimizu, Akira Mochizuki (1998). Three-Dimensional Tactile Display for the Blind. National Institute of Bioscience and Human-Technology, Tsukuba, Ibaraki, Japan.
- National Instrument Corp. (2021). Calculating Absolute Accuracy or System Accuracy. Austin, Texas, USA.
- <https://www.ni.com/en-th/support/documentation/supplemental/18/calculating-absolute-accuracy-or-system-accuracy.html>
- Nexperia (2020). Octal D-type transparent latch; 3-state. Nexperia B.V., Nijmegen, Netherlands.
- Peter Anderson (2021). Accuracy and Precision. Sophia Learning, LLC, Minneapolis, Minnesota, USA.

<https://app.sophia.org/tutorials/accuracy-and-precision--3>

Qi Zhang, Haiwei Dong, Abdulmotaleb El Saddik (2016). Magnetic Field Control for Haptic Display: System Design and Simulation. University of Ottawa, Ottawa, Canada

R. Clarke (2010). An Introduction to The Air Cored Coil. University of Surrey, Guildford, United Kingdom.

http://info.ee.surrey.ac.uk/Workshop/advice/coils/air_coils.html

Raspberry Pi Foundation (2017). Using your Raspberry Pi. Cambridge, United Kingdom.

<https://projects.raspberrypi.org/en/projects/raspberry-pi-using/0>

Raspberry Pi Foundation (2017). Physical Computing with Python. Cambridge, United Kingdom.

<https://projects.raspberrypi.org/en/projects/physical-computing/0>

Raspberry Pi Foundation (2017). Getting Started with GUIs. Cambridge, United Kingdom.

<https://projects.raspberrypi.org/en/projects/getting-started-with-guis>

Ravi Teja (2021). What is a Demultiplexer (Demux)?. ElectronicsHub, Hyderabad, Telangana, India.

<https://www.electronicshub.org/demultiplexerdemux/>

Robert H. Bishop (2002). The Mechatronics Handbook. CRC Press LLC, USA.

Robert Keim (2020). Applications of the Op-Amp: Voltage Follower Circuit. EETech Media, Boise, Idaho, USA.

<https://www.allaboutcircuits.com/video-tutorials/op-amp-applications-voltage-follower/>

Syed Hussain Ather (2020). Coil Winding Basics. Sciencing by Leaf Group, Santa Monica, California, USA.

<https://sciencing.com/coil-winding-basics-7480758.html>

Syed Zainal Abidin Syed Kamarul Bahrin, Khairul Salleh Mohamed Sahari (2016). Design and Development of a Five-Fingered Master-Slave Robotic Hand by Using Solenoid and Pressure Sensors Comparator Technology. Universiti Tenaga Nasional, Kajang, Malaysia.

Tan G.H., Surpajo B.S., Wagiran R., Sidek R. (2000). The Design Of 8-bit CMOS Digital To Analog Converter. Universiti Putra Malaysia, Serdang, Selangor, Malaysia.

- Tao Wang, Hiraku Karino, Kenta Michitsuji, Et. al.(2014). Influence of Winding Accuracy on Magnetic Field Distribution in YBCO Pancake Coil for Cyclotron Application. Waseda University, Tokyo, Japan.
- Thomas A. Manning (2003). Tension Control During The Coil Winding Process. Sipro Inc., Baltimore, Maryland, USA.
- Timothy Banas (2018). How to Calculate the Force of an Electromagnet. Sciencing by Leaf Group, Santa Monica, California, USA.
<https://sciencing.com/calculate-force-electromagnet-5969962.html>
- William J. Turkel, Adam Crymble (2012). Working with Text Files in Python. University of Hertfordshire, Hatfield, United Kingdom.
- Yi Wan, Qisong Xie (2016). A Novel Framework for Optimal RGB to Grayscale Image Conversion. Lanzhou University, Lanzhou, China.
- Yingtao Xu, Bo Tang, Baoming Li (2019). Research on Momentum Transfer in Simple Railgun. Nanjing University of Science and Technology, Nanjing, Jiangsu, China.
- Zohreh Karimi (2021). NumPy Quick Review. Kharazmi University, Tehran, Iran.